DEVELOPMENT OF CIRCULAR DRUG DELIVERY DEVICE FOR THE TREATMENT OF FUNGAL KERATITIS

Yerbolat Magazov, Bachelor of Science in Chemistry

Submitted in fulfillment of the requirements
for the degree of Master of Science
in Chemical and Materials Engineering

School of Engineering and Digital Sciences
Department of Chemical and Materials Engineering
Nazarbayev University

53 Kabanbay Batyr Avenue,
Astana, Kazakhstan, 010000

Supervisor: Levinus Hendrik Koole

April 2020

Abstract

Fungal keratitis is a dangerous infectious eye disease in which the cornea becomes inflamed and swollen, which can cause pain and redness of the eye, and without proper treatment, it can lead to loss of vision. Despite the widespread use of anti-fungal drugs, the only available forms are tablets and liquid suspensions, so the drug can only be taken orally, intravenously or in the form of eye drops. However, due to the significant drawbacks like poor biocompatibility, a short period of activity and low permeability of the intraocular drug, it is necessary to develop an alternative method that allows delivering the drug of choice to the damaged areas effectively.

This work presents the possibility of creating a drug delivery device in the form of a hydrogel ring that is capable of treating keratitis effectively. In this study, voriconazole was chosen as the antifungal drug as it is a better option in comparison with traditional antifungal agents since it showed a promising result in the treatment of yeast and filamentous fungi. Regarding the circular drug delivery device, unique hydrogel rings have been developed to have the property to swell when the drug is introduced into them. Thus, the rings hold the required amount of the drug when in contact with voriconazole while maintaining its shape. A filled ring is inserted into the eye and releases voriconazole while providing a more local and effective treatment for keratitis in a short period. In this case, patients will not have to use eye drops so often; instead, they only need to wear these devices, and during the day, the medicine will slowly release, providing an antifungal effect with enhanced bioavailability.

The biggest objective of this work was to show that a particular drug delivery device can provide drug concentration at a therapeutic level for long-duration, excluding the frequent application the eye drops. XPS and SEM-EDS analysis demonstrated that our synthesized hydrogel rings indeed consist of PVP, and voriconazole loading into the hydrogel structure was successful. In addition, the porosimetry test verified that hydrogel rings have pores with diameters 5-25 nm (54%) and 7-240 μm (46%), and a porosity of 30% provides enough space for penetration and precipitation of voriconazole crystals in the pores of the polymer rings. The drug release experiments showed that voriconazole released from the device during the two days, and after the concentration of voriconazole in PBS solution were maintained at 80 μg/mL. Another performed release study, where hydrogel rings were subjected to a new PBS solution environment, demonstrated that it could release the drug for at least ten days.

Acknowledgements

I would like to express my deepest gratitude to my supervisor, Professor Levinus Hendrik Koole, for his continuous support of my thesis work, for his immense knowledge in the field of Chemical and Biomedical Engineering, patience, great motivation and enthusiasm. His competent guidance and support helped me a lot throughout the research and writing of the thesis. I cannot imagine a better mentor and advisor for my Master's study.

Besides my advisor, I would like to express special thanks to my labmate and friend Aiym Rakhmetova for the tremendous help, stimulating discussions during the research project, and for all cheerful moments that we have had in these two years.

And last but not least, I want to thank my wonderful girlfriend, Guldana Zhigerbayeva, for her continuous support and love, which have inspired me over the past two years.

Table of Contents

Abstract 2
Acknowledgments 3
List of Abbreviations & Symbols 6
List of Figures 7
List of Tables 8

Chapter 1 - Introduction 9

1.1. Justification of the study 9
1.2. Thesis organization and objectives 11
1.3. Research hypothesis 11

Chapter 2 - Literature review 12

2.1. Antimicrobials used in the treatment of keratitis 12

2.1.1 Bacterial keratitis 12
2.1.2. Fungal keratitis..... 13

2.2. Limitations of topical drug application 14

2.2.1. Anatomy of the eye: corneal epithelium and conjunctiva 14
2.2.2. Nasolacrimal drainage system 15

2.3. Drug delivery approaches 16

2.3.1. Nanoparticles 16

2.3.1.1. Polymeric nanoparticles 17
2.3.1.2. Solid lipid nanoparticles 18

2.3.2. Contact lenses 19

2.3.2.1. Soaking method 19
2.3.2.2. Molecular imprinting 20
2.3.2.3. Coating 20

2.3.3. In Situ forming gels 21

Chapter 3 – Materials and Methods 24

3.1. Materials 24
3.2. Preparation of drug delivery device 24

3.2.1. Hydrogel formulation 24
3.2.2. Preparation of molds for hydrogel rings 25
3.2.3. Synthesis of hydrogel rings 26

3.3. Characterization of hydrogel rings 27

3.3.1. Morphological analysis 27
3.3.2. In-vitro drug release …..... 28

3.4. Spectrophotometric method for voriconazole determination in drug delivery device 28

3.4.1. Determination of optical characteristics of voriconazole 28
3.4.2. Determination of voriconazole concentration in hydrogel rings 28

Chapter 4 – Results and Discussion 30

4.1 Preparation of hydrogel rings 30
4.2. Morphological analysis 32

4.2.1. Surface characterization: X-Ray Photoelectron Spectroscopy 32
4.2.2. Surface characterization: Scanning Electron Microscopy 35
4.2.3. Pore size distribution: Mercury porosimetry analysis 37

4.3. Determination the presence of voriconazole in hydrogel rings 38
4.4. In-vitro drug release 44
4.5. Release studies 45

4.5.1. Determination of optical characteristics UV extinction of voriconazole 45
4.5.2. Determination of voriconazole concentration in hydrogel rings 47

Chapter 5 – Conclusion 51

Bibliography/References 53

List of Abbreviations & Symbols

DMSO	Dimethyl sulfoxide
DNA	Deoxyribonucleic acid
EDS	Energy-dispersive X-ray spectroscopy
FDA	Food and Drug Administration
HDDMA	1,6-Hexanediol dimethacrylate
NVP	1-Vinyl-2-pyrrolidinone
PBS	Phosphate buffer saline
PEG	Polyethylene glycol 1000
PEG-DA	Poly(ethylene glycol) diacrylate
PLGA	Poly(lactic-co-glycolic acid)
PVP	Polyvinylpyrrolidone
A	Absorbance
m_f	Mass of the mold filled with monomer solution (after heating)
m_h	Actual mass of the hydrogel rings (after washings and drying)
m_m	Mass of the mold
m_{ms}	Mass of the mold filled with monomer solution (before heating)
m_{th}	Theoretical mass of the hydrogel rings
V_t	Total volume
V_v	Volume of void space
λ_{max}	Maximum absorption wavelength
ϕ	Porosity

List of Figures

Figure 1.1. An example of fungal keratitis, where corneal lesion is prominent..... 9
Figure 2.1. Nasolacrimal system anatomy 15
Figure 2.2 Drug delivery approaches for the keratitis treatment 16
Figure 3.1. Schematic representation of Teflon mold 25
Figure 3.2. Teflon molds with various diameters and depth sizes 26
Figure 4.1. Hydrogel rings with various diameter and height..... 31
Figure 4.2. Polymerization of vinylpyrrolidone 32
Figure 4.3. Chemical structure of voriconazole 33
Figure 4.4. XPS spectra of hydrogel rings without voriconazole (group B) 33
Figure 4.5. XPS spectra of hydrogel rings with loaded voriconazole (group A) 34
Figure 4.6. XPS spectra of hydrogel rings..... 34
Figure 4.7. Schematic representation of hydrogel ring..... 35
Figure 4.8. SEM images of hydrogel rings without voriconazole loading..... 36
Figure 4.9. SEM images of hydrogel rings with voriconazole loading..... 37
Figure 4.10. Mercury porosimetry analysis of hydrogel rings 38
Figure 4.11. The hydrogel rings under UV light: group B (left) and group A (right) 39
Figure 4.12. EDS mapping of SEM analysis of “drug-loaded” hydrogel ring (top surface) ... 40
Figure 4.13. EDS mapping of SEM analysis of “loaded” hydrogel ring (bottom surface) 41
Figure 4.14. EDS mapping of SEM analysis of “unloaded” hydrogel ring (top side) 42
Figure 4.15. EDS mapping of SEM analysis of “unloaded” hydrogel ring (bottom side) 43
Figure 4.16. In vitro test on *Aspergillus*: 10 wt.% PEG (left) and 20 wt.% PEG (right) 45
Figure 4.17. UV absorption spectra of voriconazole 46
Figure 4.18. Calibration curve of voriconazole solutions 47
Figure 4.19. Cumulative release of voriconazole from the hydrogel ring (OD=10 mm, ID=6 mm, H=0.8 mm) for 2 hours (A) and 5 days (B) 48
Figure 4.20. Release of voriconazole from the hydrogel ring (OD=10 mm, ID=6 mm, H=0.8 mm) for 10 days 49

List of Tables

Table 2.1: Drugs used in the treatment of keratitis 14
Table 2.2. Nanoparticles for the drug delivery to treat keratitis 17
Table 2.3. Contact lenses for the drug delivery to treat keratitis 21
Table 2.4. Hydrogels for the drug delivery to treat keratitis 22
Table 3.1. List of chemicals used in hydrogel synthesis with their characteristic properties... 24
Table 3.2. Mold dimensions 25
Table 3.3. Specification of hydrogel rings 27
Table 4.1. Dependence of hydrogel ring's mass on reaction time 30
Table 4.2. Comparison of spectrophotometric results with the current method 46
Table 4.3. Optical characteristics of voriconazole 47

Chapter 1 – Introduction

1.1. Justification of the study

The condition of an eye when the cornea (a membrane which is covering the eye's pupil and iris) is inflamed or swollen can be defined with the term called keratitis [1]. Keratitis can cause pain and redness of the eye, and without subsequent proper treatment, it may lead to vision loss [1]. According to Jurkunas et al. [1], two types of ocular disease are present nowadays, namely infectious and non-infectious keratitis. Keratitis can appear in the life of a regular person due to some eye injuries or infections, neglected state of the eye (dry eyes) and the improper wearing of contact lenses (most common nowadays) [1, 2]. The scope of this research will cover only the infectious type of keratitis, namely the fungal one.

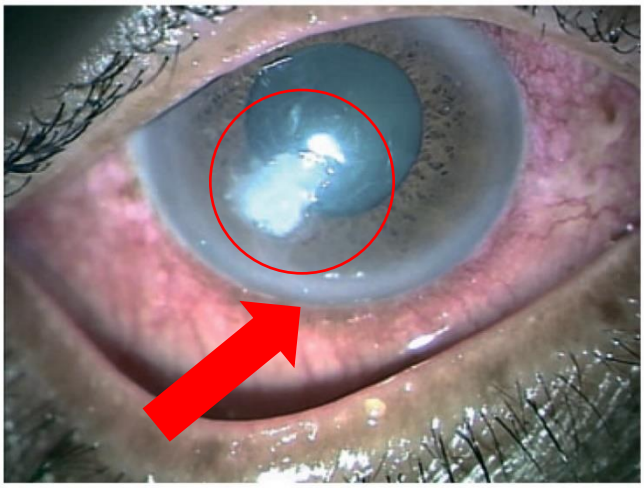

Figure 1.1. An example of fungal keratitis, where the corneal lesion is prominent (taken from [3]). Arrows represent the opacification area.

Over the last decade, there is a markedly increasing trend of fungal keratitis appearance in different geographic regions, including countries like China, USA, India, and Australia [2]. For example, considering all cases related to the infectious type of keratitis, the fungal one shows 39% in India, 61.9% in Northern China, and 6-20% in the USA [2, 3]. There are three main factors that cause this ocular disease to appear in these countries. The first factor is the regular use of topical corticosteroids, which, in turn, leads to high resistance to antimicrobials. The second one is ocular trauma, where it creates potential spaces for microorganism invasion. The last factor is associated with wearing contact lenses for an extended period of time-overnight [1-4]. The combination of these factors leads to the penetration of fungi into the inner layers of the cornea, where the latter, in turn, initiates an immune response with subsequent

inflammation. Figure 1.1 shows that fungal keratitis may lead to tissue necrosis and the opacification of the surrounding area on the corneal surface.

Fungal keratitis is a dangerous disease as it may lead to total unilateral blindness. Therefore, effective treatment and methodology should be developed. Modern methods of treatment are mostly ineffective for several reasons: poor bioavailability of the drug due to low corneal permeability, drug resistance and insensitivity of fungi, as well as difficulties with sustained release of the drug [5]. It is essential to mention at this stage that keratitis is considered as an intractable disease. Therefore, therapeutic keratoplasty is often used in combination with drug therapy to increase the effectiveness of a course of keratitis treatment [6]. However, this procedure has its drawbacks in the face of sophisticated surgical techniques and the possibility of a deterioration in vision [7]. As can be seen, currently, the treatment remains as challenging, risky, and long-term therapy.

Voriconazole is an antifungal agent that is a better option in comparison with traditional antifungal agents, since recently, it showed a promising result in the treatment of yeast and filamentous fungi infection [8]. Although it is a popular type of therapy against severe fungal infections, the only available forms are tablets and liquid suspension, so the drug can only be taken orally, intravenously or in the form of eye drops [8]. The main disadvantage of such oral administration is the time since this method requires an extended treatment period [4, 8]. For example, to cure the *Esophageal candidiasis*, the candidates (patients) should use voriconazole for two weeks at least [4]. Consequently, this type of long course treatment may cause problems associated with fever, rash, respiratory distress, transient visual disturbances and peripheral edema [8-9]. Thus, to minimize side effects and increase drug concentration at damaged regions, only eye drops and drug injection should be used [9].

Considering the fact that drug injection into the eye is associated with its complexity and possible vision problems, it is clear that antifungal eye drops can be considered as the only option in keratitis treatment [1, 9]. Under the clinical conditions, eye drops are commonly used as they are non-invasive and easy-to-use therapeutic approaches while remaining cost-effective [1]. However, this method also has some significant drawbacks: low solubility and poor bioavailability due to poor dispersion and low intraocular drug permeability [5]. It worth mentioning that it has a short period of activity as only 1-10% of the drug volume reaches the damaged target areas because most of the voriconazole dosage is removed by the movement of the eyelids (blinking and flow of tear fluid) [5]. Another problem associated with this method

is its poor bioavailability meaning that voriconazole should be injected frequently into the eye. For example, Prajna [9], in his experiments, applied these eye drops to patients every 4 hours. Also, it is worth mentioning that under clinical conditions, it is difficult to follow and control the methodology as frequent high daily doses of voriconazole can result in some side effects that were mentioned earlier.

1.2. Thesis organization and objectives

Taking into consideration the above-stated problems associated with the treatment of fungal keratitis and considering the fact that the method is very ineffective in terms of cost of the drug, treatment time and overall performance, the main objective of this work is to design and construct a polymer device that is capable of delivering a drug of choice to a target ocular surface for effective treatment of fungal keratitis. The polymer device in the form of a ring has the property to swell when the drug is introduced into them. Thus, the ring hold the required amount of the drug when in contact with it while maintaining its shape. A filled ring is inserted into the eye and releases the drug while providing a more local and effective treatment for keratitis in a short period. In this case, patients will not have to use eye drops so often; instead, they only need to wear these devices, and during the day, the medicine will slowly release, providing an antifungal effect with enhanced bioavailability. Regarding the shape of the device, the circular form was selected as it is anticipated that there will be practically no tear flow in the inner region of the ring, exactly at the site of the infection. The absence of tear flow in the center of the ring may lead to enhanced bioavailability as the drug would not be washed out.

The methodology of this project can be divided into three main parts, namely (1) preparation of drug delivery device, including the formulation of hydrogel and its synthesis; (2) characterization of hydrogel rings, namely morphological and spectrophotometric analysis, and (3) in vitro drug release experiments.

1.3. Research hypothesis

- The synthesized polymer rings could show the required mechanical property, namely, flexibility – the most essential feature for the ocular device.
- The hydrogel rings could have a porous structure that allows voriconazole crystals to penetrate and precipitate in the polymer matrix.
- The circular drug delivery device could achieve two primary goals, namely sustained release of the drug and enhanced bioavailability.

Chapter 2 - Literature review

As it was said earlier, fungal keratitis is a dangerous disease as it may lead to total unilateral blindness. Therefore, effective treatment and methodology should be developed. Modern methods of treatment are mostly ineffective due to several reasons, including drug resistance and insensitivity of infections, as well as difficulties with a sustained release of the drug [7-9]. Considering the fact that drug injection into the eye is associated with its complexity and possible vision problems, it is clear that eye drops can be considered as the only option in keratitis treatment [1-3]. It should be noted that many studies were done to create a drug delivery system to provide effective treatment. However, they did not find practical and clinical applications [10-14]. Therefore, this work was done to find out and systemize the recent studies and discoveries in this area and find the most common methods that show some promising results. Notably, this paper considered the available antimicrobials used against each type of keratitis and novel approaches for antimicrobials delivery to the corneal surface. Besides, the scope of this research was limited only by treatments that were used against bacterial and fungal keratitis.

2.1. Antimicrobials used in the treatment of keratitis

Approximately 30,000 cases of keratitis are reported annually only in the US [10]. The treatment of infectious keratitis mostly requires therapy, which includes the application of aggressive antimicrobials. An overview of such antimicrobials used in the treatment of infectious keratitis was discussed in detail below and summarized in Table 2.1.

2.1.1. Bacterial keratitis

Various types of pathogens can cause bacterial keratitis, where a geographic location plays a crucial role. For example, the most common pathogens found in the US are *Serratia, Pseudomonas, Streptococci* and *Staphylococci* [7, 10]. According to the American Academy of Ophthalmology [10], the bacterial acquired cases are mostly treated with antibiotic therapy. Therapy typically includes either the application of fluoroquinolones or fortified aminoglycosides (antibiotics) [11]. According to McDonald et al. [11], *Staphylococcus aureus* is the most abundant infection that causes keratitis, and fortified vancomycin was selected as the drug choice. For this type of keratitis, the usual practice is to combine Cefazolin/Ceftazidime (50 mg/mL) with Gentamicin/Tobramycin (14 mg/mL) in order to

provide an adequate cure against bacteria for both gram-positive and gram-negative one [10, 11].

Fluoroquinolones are another type of antibiotics that inhibit topoisomerase II and IV enzymes [12]. They are essential for DNA replication and transcription. Therefore, inhibition of these enzymes prevents the growth of bacteria. The most common fluoroquinolones are ciprofloxacin, ofloxacin, levofloxacin and moxifloxacin [12].

2.1.2. Fungal keratitis

Fungal keratitis is mostly caused by *Aspergillus, Fusarium* and *Candida* [13, 14]. The only FDA approved antifungal medication is Natamycin, which belongs to the class of polyenes and is very effective against *Aspergillus, Fusarium* and *Candida* [13, 14]. Others, like Amphotericin B, only works against *Candida* [14]. Amphotericin B is available as a 0.15% solution, whereas Natamycin is provided as a 5% ophthalmic solution. The working principle of polyenes is that they bind to ergosterol (sterol that was found in the plasma membrane of fungi) and produce pores, which affect the membrane permeability. As a result, vital cellular molecules escape the cell causing fungal death [14].

Another class of antifungal drugs is azoles, which include econazole, fluconazole, miconazole and voriconazole [13]. In comparison with polyenes, azoles inhibit the synthesis of ergosterol by blocking 14-α-sterol demethylase enzyme; however, each drug shows some difference in their efficacy [13]. For instance, voriconazole is highly effective against *Aspergillus, Fusarium* and *Candida*, whereas miconazole only works against *Candida.* In the study conducted by Muller [14], natamycin demonstrates superiority in comparison with azole antifungal drugs.

A novel class of antifungal drugs that recently discovered is Echinocandins [15]. This drug acts as an inhibitor of glucan (a crucial component of the cell wall). The fungicidal effect was achieved by the alteration of the glucan synthesis, which in turn affects the structural integrity of the cell wall. In clinical studies, Micafungin (echinocandins) show efficacy against *Candida* comparable to fluconazole [15, 16].

Table 2.1. Drugs used in the treatment of keratitis

Type of keratitis	Drug		Formulation	FDA approval	Ref.
Bacterial	Fortified antibiotics	Cefazolin/ Ceftazidime	5% solution	Yes	[10]
		Gentamicin/ Tobramycin	1.4% solution		[10]
		Vancomycin	1.5-5% solution		[17]
	Fluoroquinolones	Ofloxacin	0.3% solution	Yes	[12]
		Gatifloxacin	0.5% solution		[12]
		Ciprofloxacin	0.3% solution		[12]
		Moxifloxacin	0.5% solution	Off-label	[12]
Fungal	Polyenes	Amphotericin	0.15% solution	Off-label	[14]
		Natamycin	5% solution	Yes	[14]
	Azoles	Econazole	1% solution	Off-label	[18]
		Fluconazole	2% solution		[19]
		Miconazole	2% solution		[20]
		Voriconazole	1-2% solution		[9, 21]
	Echinocandins	Micafungin	1% solution	No	[15, 16]

Note: “Off-label” means the drug was used in a manner not specified in the FDA-approved label. The label itself is a written report that contains detailed instructions of drug’ uses and doses.

2.2. Limitations of topical drug application

The successful treatment of keratitis depends on two significant factors, namely adequate amounts of drugs on the surface of the cornea and the optimal duration of therapy. The traditional method of drug-delivering is the instillation of eye drops. Despite the fact that eye drops provide an easy administration, they usually demonstrate a poor bioavailability due to low corneal permeability and rapid nasolacrimal drainage. As a result, a frequent application of eye drops is required to reach a certain therapeutic level. However, this action leads to significant fluctuation in drug dosage on the eye surface as there will be a short period of overdosing, followed by a long period of underdosing [22].

2.2.1. Anatomy of the eye: corneal epithelium and conjunctiva

The cornea consists of 6 layers of epithelium cells, which form a package that creates a barrier against drug permeation [23]. The cells are packed closely together, creating tight junctions. These tight junctions are mainly composed of two transmembrane proteins, namely

claudin and occludin. The presence of joints delays the permeation process making it difficult for molecules (larger than 5000 Da) to pass through the cornea [23].

Conjunctiva, on the other hand, is a clear, thin membrane that covers the sclera and the inner surface of the eyelids [23]. The structure of the conjunctiva is similar to the cornea, and it consists of 6-7 layers of epithelium cells, which are connected by tight junctions. This, in turn, creates a barrier for molecules that have a mass larger than 20,000 Da [23].

2.2.2. Nasolacrimal drainage system

Nasolacrimal drainage is the major factor resulting in poor ocular bioavailability and short residence time of administered drugs [23, 24]. The average volume of human tear is approximately 7 µl, and this value is kept constant by a continuous tear production. Only 3 µl of other fluids can be combined with the tear without causing destabilization. However, the tear volume increases as eye drops applied, causing excessive fluid containing drug flow through the canaliculi into the nasolacrimal duct (Figure 2.1) [24]. Therefore, the drug has a short residence time of approximately 2 minutes on the ocular surface, and only about 5-10% of the drug is absorbed into the cornea [9, 21]. Also, as the tear flows into the nasolacrimal duct, the drug can be absorbed into the bloodstream. In this scenario, the instillation of eye drops can result not only in the drug wastage but also may cause various side effects. Examples of such systemic side effects for antimicrobial eye drops include dyspnea and chest pain for natamycin or dizziness and nausea for fluoroquinolones [24].

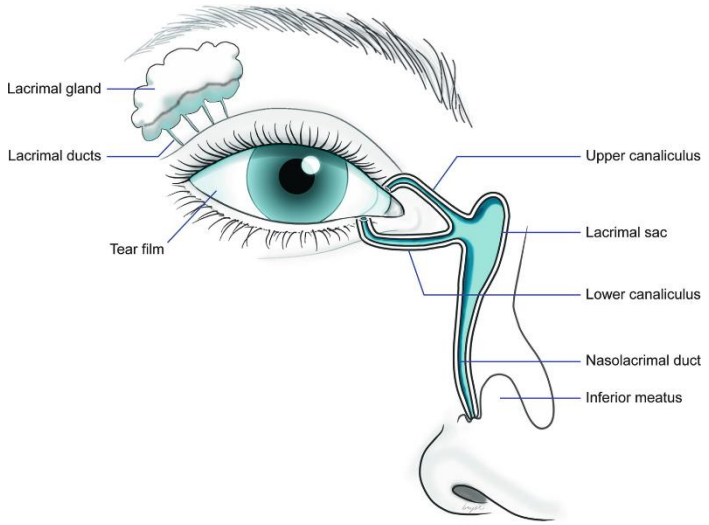

Figure 2.1. Nasolacrimal system anatomy (taken from [25])

2.3. Drug delivery approaches

Various new drug delivery approaches are developed to achieve two primary goals, namely sustained release of the drug and enhanced bioavailability. In this section, three main strategies (nanoparticles, contact lenses and gels) will be discussed and evaluated in terms of device working principle, residence time at the eye surface and drug permeation ability.

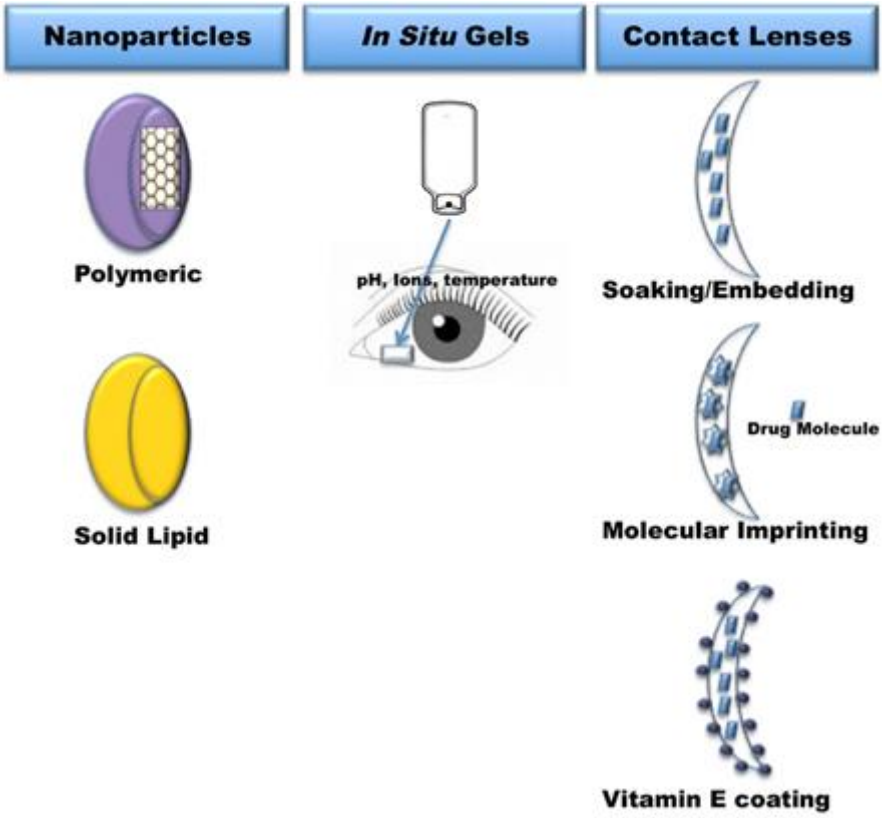

Figure 2.2. Drug delivery approaches for the keratitis treatment (taken from [26]). In all three cases, the devices were preloaded with the drug.

2.3.1. Nanoparticles

For the past decade, nanoparticles show an increasing trend in drug delivery due to their unique properties [27-29]. Among all tested nanoparticles, the optimal diameter size for drug delivery is 10-100 nm [27]. Larger nanoparticles became a subject of phagocytosis, whereas smaller particles have faster renal clearance. Nanoparticles have a high surface area/mass ratio, which allows them to transport a large number of drug molecules [28]. In addition, these nanoparticles preloaded with the drug can be rapidly taken up by the cells due to their small size. Drug molecules can be embedded into nanoparticles through various techniques, which include chemical conjugation, entrapment, surface adsorption and encapsulation [29].

Additional modification in their surface structure allows to control and enhance the diffusion and release rate [27-29]. The recent advances in using nanoparticles as a drug delivery device were summarized in Table 2.2

Table 2.2. Nanoparticles for the drug delivery to treat keratitis (application of various drugs and different models where they have been used successfully)

Nanoparticle type		Drug	*In vitro* model	*In vivo* model	Notes	Ref.
Polymers	Eudragit	Amphotericin	Dialysis membrane	Rabbit	A slight increase in residence time and corneal penetration	[30]
		Gatifloxacin				[31]
	Chitosan in combination with anionic polymers	Amphotericin	Goat cornea and dialysis membrane	Rabbit	Alginate, lecithin and polylactic acid were used with chitosan.	[32, 33]
		Econazole				[34]
		Natamycin				[35]
	PLGA	Levofloxacin	Goat cornea	Rabbit	Extension of the corneal residence time	[36]
Solid lipids		Gatifloxacin	Goat cornea	Rabbit and chorioallantoic membrane	A significant increase in residence time and corneal penetration	[37]
		Tobramycin				[38]

2.3.1.1. Polymeric nanoparticles

Among all polymeric nanoparticles, chitosan and PLGA are considered to be the most effective method of delivering the antimicrobial drugs [36, 37]. Gupta et al. [36] demonstrated an extended release as well as enhanced bioavailability of PLGA nanoparticles in their research work. For example, in vitro experiments on goat corneas showed that PLGA nanoparticles loaded with drugs demonstrated a 24-hour release of levofloxacin compared to only 6 hours in case of ophthalmic formulations present in the market [36]. In vivo experiments on rabbits showed that this formulation has a prolonged residence time on the cornea. In addition, these nanoparticles demonstrated stability for several months at room temperature and non-irritation in the study with the chorioallantoic membrane of the egg [37].

The second type of polymeric nanoparticles is chitosan-based one, which is a polysaccharide synthesized from crustacean shells [38]. It shows non-toxic and biodegradable properties to the eye [38]. Since chitosan a hydrophilic polymer, it has a limited capacity to intake hydrophobic drugs [32-35]. The formulation of amphiphilic chitosan nanoparticles was achieved by the combination with other anionic polymers [32-35]. For example, the combination of chitosan and alginate showed a burst release of the drug during the first hour and a more gradual release for 24 hours during the in vitro test on dialysis membranes [38]. Another experiment carried out by combining chitosan and polylactic acid to incorporate it with the highly hydrophobic drug, amphotericin B [32]. The results of in vivo testing on rabbits showed a 2 times increase in residence time compared to the ophthalmic solution of amphotericin B [32]. Another research group tested a combination of chitosan and cyclodextrin nanoparticles for econazole delivery [33]. In vitro tests demonstrated a controlled release of the drug for the 8 hours in comparison with 2 hours release of commercially available econazole. Furthermore, a prolonged anti-fungal activity was observed in the case of chitosan/cyclodextrin nanoparticles, namely a more than 25% increase for 8 hours release against the only 4-hours action of the drug for econazole solution alone [34].

The third type of polymeric nanoparticles is eudragit nanoparticles, which are used to deliver either amphotericin B or gatifloxacin [30, 31]. In vitro and in vivo studies showed that bioavailability of either drug was not increased in combination with these nanoparticles; however, the sustained release of gatifloxacin was achieved [31].

Overall, the chitosan nanoparticles are considered to be the most promising method of drug delivery compared to PLGA and eudragit nanoparticles [30, 31, 36]. Chitosan nanoparticles showed an improvement in bioavailability and residence time of the drug as these two factors are crucial for the effective treatment of keratitis [36].

2.3.1.2. Solid lipid nanoparticles

In the early 1990s, solid lipid nanoparticles were first examined, and they demonstrated an advantage in terms of non-toxicity as the preparation of these nanoparticles required the use of lipids, which are biodegradable and biocompatible [39, 40]. Solid lipid nanoparticles consist of lipid core, which is solid at human body temperature [39]. A lipophilic drug that is combined with these nanoparticles slowly releases as the lipid core dissolves the drug over a certain period. The main advantage of using lipid nanoparticles is that they provide protection for the drug (no degradation), improve the adherence to the eye layer, and increase the residence time

[39]. Several formulations of lipid nanoparticles with various antimicrobials have been tested to measure the release time and transcorneal bioavailability [37-39]. For example, the research group lead by Cavalli et al. [38] prepared the nanoparticles synthesized from epikuron 200 (lipid) and stearic acid with the addition of tobramycin into the formulation. In vivo experiments on rabbits resulted in a time increase for the drug to reach its maximum concentration compared to the results observed from eye drops [38]. Another experiment that was done with nanoparticles comprised of compritol (lipid), stearic acid and gatifloxacin (drug) demonstrated a gradual release of the drug [37]. Compared to the regular eye drops of 0.3% gatifloxacin solution, the lipid nanoparticles showed a 4-fold increase in bioavailability of the drug and a 2-fold increase in C_{max} (the peak concentration of gatifloxacin) [37]. As can be seen from the above stated in-vitro and in-vivo results, only bacterial keratitis has been treated with this approach.

2.3.2. Contact lenses

Contact lenses are made of hydrogels and provide the advantage of using them on the cornea without any side effects [41]. As millions of people all over the world wear contact lenses, the biocompatibility, as well as the safety of these devices, are well established. Several approaches were tested to use contact lenses as ocular drug delivery devices, including surface modifications, soaking contact lenses in drug solution, and creating a reservoir for a drug by merging two lenses [41].

2.3.2.1. Soaking method

The simple method of soaking the commercially available contact lenses in a drug solution has shown a limited success due to the fact that the drug rapidly released from this device without demonstrating the sustained release. Hui et al. [42], tested different silicone-based contact lenses from various brands using ciprofloxacin as a drug of interest. Most of the drug was released in the first 10 minutes, demonstrating that conventional contact lenses cannot be used as a drug delivery device [42]. The same procedure was used by Phan et al. [43], where they used the same silicone hydrogel lenses to test fluconazole and natamycin release. The drug was released from the lenses in one hour when placed in PBS solution, demonstrating a burst and not sustained release. However, a more recent study conducted by Bajgrowicz et al. [44] revealed that previous experiments from various research groups used a wrong model and not ideal conditions. Bajgrowicz et al. [44] designed an eye model that mimics the blinking condition and tear flow of the human eye. Using this artificial eye, they showed a 24-hour

sustained release of moxifloxacin and ciprofloxacin. This phenomenon can be explained by the fact that the drug of interest is released from the device by simple diffusion and exposing contact lenses to large volumes of artificial tear fluid results in burst release. This statement was further supported by Busin and Spitznas [45], where contact lenses soaked in gentamicin results in maintaining therapeutic drug concentrations for three days.

2.3.2.2. Molecular imprinting

The most recent method of achieving sustained drug release is molecular imprinting. Molecular imprinting is a technique used to create template-shaped cavities in the matrix of a polymer with a memory of the template molecules to be used in molecular recognition. This method involves two main components, namely, polymeric hydrogel mixture (monomers) and the drug that should be delivered [46]. The drug molecule is then coated with a hydrogel, which was initiated by the polymerization reaction. Different types of monomers, as well as their ratio, can greatly affect the hydrogel's transparency, oxygen diffusion and water content. These three factors dictate whether the produced contact lens will be suitable or not. The research group of Hui et al. [46] tested ciprofloxacin drug release from molecularly imprinted hydrogel lenses, and they showed that these lenses could provide an 8 hour of sustained release of ciprofloxacin. Additionally, these devices were tested on rabbits to cure *Pseudomonas* keratitis, where Hui et al. [46] demonstrated the effectiveness of contact lenses compared to the regular eye drops.

2.3.2.3. Coating

Another strategy to obtain a prolonged and sustained release of the drug is coating the contact lenses with another material. However, it should be noted that a coating material should not interfere with oxygen and water permeability. Therefore, vitamin E was selected as the perfect coating material since it shows promising results [47]. Three types of commercially available contact lenses were coated with vitamin E, where fluconazole loaded into the device as an antifungal drug [47]. The uncoated lenses released the drug in 2-8 hours, whereas the vitamin E coating extended this number for one week. Peng, Kim & Chauhan [48] added that vitamin E was not leached out during the storage, demonstrating that these coated contact lenses have an appropriate shelf-life. Another study conducted by Paradiso et al. [49] indicated that levofloxacin was released from vitamin E coated contact lenses in 50-100 hours.

Table 2.3. Contact lenses for the drug delivery to treat keratitis (application of various drugs and different models where they have been used successfully)

Loading method	Drug	Model	Notes	Reference
Soaking	Fluconazole	Drug was released in stirred solution	No sustained-release effect	[43]
	Ciprofloxacin			[42, 44]
	Natamycin			[43]
	Gentamicin		Maintained drug concentrations for 3 days	[45]
Molecular Imprinting	Ciprofloxacin	Rabbit model: *Pseudomonas* keratitis	Effect compared to eye drops	[46]
Vitamin E coating	Fluconazole	Drug was released in stirred solution	Drug released for 50 hours – 7 days	[47, 48]
	Levofloxacin			[49]

2.3.3. In Situ forming gels

By definition, hydrogels are cross-linked networks of synthetic or natural polymers that have the ability to absorb a certain amount of water to achieve the consistency of a gel [50]. Due to the high viscosity property of hydrogels, the washout from the ocular surface can be prevented, which in turn provides the sustained drug release and increases the residence time at the surface of the eye [50]. The release kinetics can be modified in different ways starting from altering the polymer formulation to change the porosity and the degree of cross-linking. As it was said, the hydrogels can be synthesized from either natural (chitosan, dextran, xanthan gum, starch, hyaluronic acid, cellulose) or synthetic polymers (polyvinyl alcohol, polyacrylic acid, polymethacrylate, polyacrylamide, polyethylene glycol) [51]. The advantage of natural polymers is their non-toxicity and biodegradability. However, they often experienced weak mechanical strength. Synthetic polymers, on the other hand, have high reproducibility and balanced mechanical properties but suffer from low biodegradability and biocompatibility [50, 51].

Several studies were reviewed where in situ hydrogels have been tested for ophthalmic drug delivery [52-56]. For example, Shastri et al. [52] combined sodium alginate, poloxamer and xanthan gum to develop hydrogel, which is sensitive to pH and temperature changes. In this study, they found a sustained release of moxifloxacin (antibacterial drug) in sheep's ocular surface. In addition, the hydrogel was adhesive enough and transparent, so this method does

not interfere with the normal vision. Another experiment made by Nanjwade et al. [53] demonstrated an 8-hour release performance of sparfloxacin in the dialysis membrane compared to 2 hours found in the eye drops. This time the authors combined three different sensitive polymers, namely sodium alginate (ion), polyox (pH) and poloxamer (temperature).

Recent studies show that it is beneficial to combine in situ forming gels with other drug delivery approaches to enhance the residence time of antimicrobials on the ocular surface [54]. Even though chitosan alone can deliver the drug for 12 hours, combination with PLGA nanoparticles can further increase its residence time on cornea [54].

The above-stated experiments mostly performed on the cornea in order to treat bacterial keratitis. However, in the case of fungal keratitis, most studies were conducted by using in situ hydrogels synthesized from synthetic polymers [55]. The hydrogels were loaded with antifungal agents such as naftifine and miconazole and tested in vitro, showing a sustained release profile [55]. However, these studies were lack of information about the irritancy and toxicity, which in turn can limit their clinical application.

Table 2.4. Hydrogels for the drug delivery to treat keratitis (application of various drugs and different models where they have been used successfully)

Hydrogel	Drug	*In vitro* model	*In vivo* model	Notes	Reference
Alginate	Gatifloxacin	Sheep cornea	Rabbit and chorioallantoic membrane	Sustained drug release for 8 hours	[57]
	Ciprofloxacin				[52]
	Moxifloxacin				[52, 53]
Poloxamer	Gatifloxacin	Sheep cornea	Rabbit and chorioallantoic membrane	Sustained drug release for 12 hours	[57]
	Ciprofloxacin				[53]
	Moxifloxacin				[52, 53]
Chitosan	Sparfloxacin	-	Rabbit	Sustained drug release for 12 hours	[56]

Taking into consideration the above-discussed drug delivery approaches, namely nanoparticles, in situ forming polymers and contact lenses, the latter drug delivery system has gained our attention since contact lenses provide the advantage of using them on the cornea without any side effects. As millions of people all over the world wear contact lenses, the biocompatibility, as well as the safety of these devices, are well established. Although nanoparticles and in situ forming gels demonstrated promising results as drug delivery systems, they also experienced some disadvantages: weak mechanical strength in case of in situ forming

gels and fast clearance or phagocytosis of nanoparticles on the ocular surface. In this work, the method of soaking contact lenses in the drug solution was considered and further modified, namely contact lenses were redesigned. In the studies conducted by Hui et al. [42], Phan et al. [43], Bajgrowicz et al. [44], and Busin and Spitznas [45], they soaked commercially available contact lenses in the drug solution, so the drug crystals were deposited only on the surface of the lens. However, in this work, the hydrogel (contact lenses) was reformulated and synthesized in the form of a ring, namely the porosity level was increased so that drug particles can penetrate the hydrogel matrix and deposited there as well. This concept, in turn, would create an extended release of the drug from this circular device.

Chapter 3 – Materials and Methods

3.1. Materials

All chemical reagents used in this work were of analytical reagent grade and used without any prior purification. The experimental procedure includes four main sections, which are hydrogel formulation and its synthesis, drug delivery device preparation, hydrogel rings characterization, and release rate experiments. For hydrogel synthesis, 1-vinyl-2-pyrrolidinone (≥ 99%), polyethylene glycol 1000, 1,6-hexanediol dimethacrylate (≥ 90%), and tert-butyl peroxy benzoate (98%) were provided by Sigma-Aldrich. During the preparation of the drug delivery device, voriconazole (99%) was purchased from Hyper Chemicals and used as an antifungal drug. In order to dissolve voriconazole (powder) and dilute it, dimethyl sulfoxide (≥ 99.9%) and phosphate buffer saline (tablets) were used, respectively. Both reagents were received from Sigma-Aldrich.

3.2. Preparation of drug delivery device

3.2.1. Hydrogel formulation

The vital element of this project is to prepare a hydrogel that would have required mechanical and morphological properties that are essential to intake our antifungal drug (voriconazole). The first step is to synthesize a hydrogel from a pool of initial monomer cocktails. Through trial and error, the formulation of hydrogel was established, and it includes 1-vinyl-2-pyrrolidinone (NVP), 1,6-hexanediol dimethacrylate (HDDMA), tert-butyl peroxy benzoate (TBPB) and polyethylene glycol (PEG) 1000.

Table 3.1. List of chemicals used in hydrogel synthesis with their characteristic properties

Reagent	Characteristic property
1-vinyl-2-pyrrolidinone (NVP)	Main monomer
1,6-hexanediol dimethacrylate (Cross-linker)	Difunctional monomer which was used for crosslinking in the polymer architecture
tert-butyl peroxy benzoate (Initiator)	The radical initiator used in the polymerization reaction
Polyethylene glycol 1000 (PEG)	Compound that is added to create pores in the polymer structure. PEG is very soluble in water, so later it can be washed out with water, leaving the “space” in the structure.

1.15 g of NVP, 0.5 g of HDDMA, 0.35 g of TBPB and 0.2 g of PEG were precisely weighed on an analytical balance and transferred respectively into 22 mL vial where they were mixed to obtain a homogeneous solution (no solvent was used). Since PEG is a solid compound, it takes 10-15 min to dissolve in the following monomer cocktail.

3.2.2. Preparation of molds for hydrogel rings

The molds required for the synthesis of hydrogels rings were made by collaboration with NURIS (Nazarbayev University Research & Innovation System). Teflon was selected as a material of choice for the molds since the hydrogel rings will not stick to the surface of mold after the polymerization reaction. The Teflon bricks were cut and processed on milling machine DMG MORI (DMU 50 model) with high precision according to the scheme illustrated in Figure 3.1. A small incision (1 cm) near the circular cavity on Teflon molds was made to remove hydrogel rings easily without doing any damage to it.

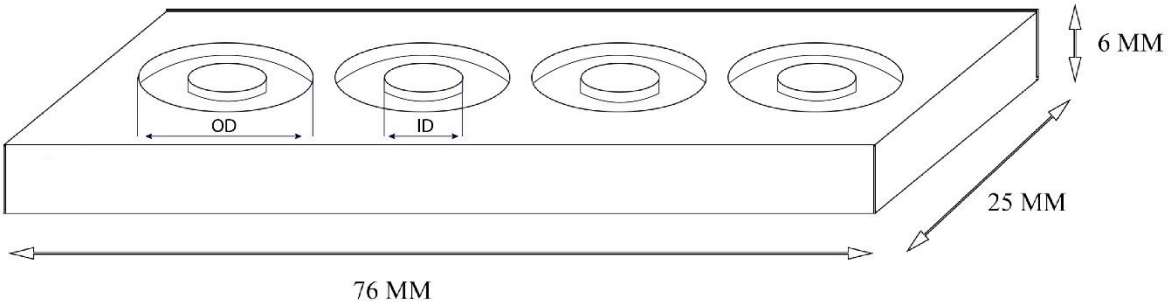

Figure 3.1. Schematic representation of Teflon mold.

Table 3.2. Mold dimensions

Outer diameter (OD), mm	Inner diameter (ID), mm	Depth, mm	Length, mm	Width, mm	Height, mm
10	6	1	76	25	6
10	6	0.8	76	25	6
9	5	1	76	25	6
9	5	0.8	76	25	6

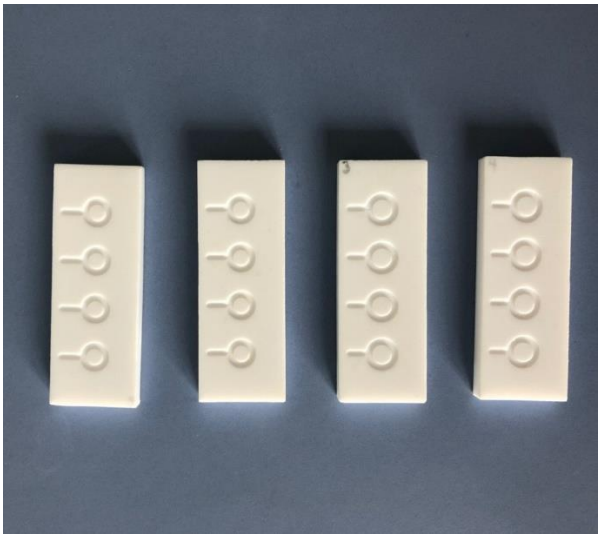

Figure 3.2. 4 types of Teflon molds with various diameters and depth sizes (obtained after processing on milling machine).

Note: A small incision (1 cm) near the circular cavity on Teflon molds was made to remove hydrogel rings easily without doing any damage to it.

3.2.3. Synthesis of hydrogel rings

Monomer cocktail was transferred with a pipette into the circular cavity of the mold. Then these molds with monomer solution in it were left in the oven for 40 minutes at 80°C. After, the hydrogel rings were carefully taken out with the help of a small needle and put into the vial with water. 7-10 washings with 20 ml of water were required to get rid of unreacted chemicals and dissolve PEG. The washed rings were left on the bench for 24 hours to dry.

On the next day, after 24 hours, the rings were transferred into the 22 mL vial containing a voriconazole solution. The voriconazole solution itself was made by dissolving 1 g of voriconazole powder in 5 g of DMSO, obtaining in total 4.55 ml of voriconazole solution and a concentration of 0.63 M. The rings were left in voriconazole solution for 24 hours. After this time interval, 7-10 washings with 20 ml of water were required. Crystallization was seen. The washed rings were transferred into the 22 mL vial containing distilled water and left there for 24 hours to get rid of the DMSO solvent. After this period, the hydrogel rings were again washed 7-10 times with 20 ml of distilled water and left on the bench for 24 hours to dry at room temperature.

As a result, two groups of hydrogel rings with various sizes were produced, namely rings with and without voriconazole in it (Table 3.3).

Table 3.3. Specification of hydrogel rings obtained after the polymerization reaction

	Outer diameter (OD), mm	Inner diameter (ID), mm	Height (H), mm	Voriconazole
Group A	10	6	1	Present
	10	6	0.8	
	9	5	1	
	9	5	0.8	
Group B	10	6	1	Not present
	10	6	0.8	
	9	5	1	
	9	5	0.8	

3.3 Characterization of hydrogel rings

3.3.1. Morphological analysis

After successful synthesis of hydrogels, it is crucial to view the surface as well as the inside of the polymer using microscopy instruments, particularly scanning electron microscopy (SEM). One sample from groups A and B, particularly two sides of the rings (upper and bottom surface), were studied with SEM (Cross Beam 540, Carl Zeiss) to examine the presence of pores, and to measure their size. In addition, mercury intrusion porosimeter (POREMASTER 60, Quantachrome Instruments) was used to measure the pore size and pore volume distribution. In the mercury pore size measurement technique, the liquid was penetrated through the pores under sufficient pressure (0.2-60000 psi). By measuring the volume of introduced by mercury, the pore volume was measured within the polymer structure

XPS spectroscopy was used to analyze the chemical composition of hydrogel rings (i.e., the elements that are present on the top surface). Hydrogels from groups A and B were sent to Guangzhou company in China, where they analyzed via K-Alpha X-ray Photoelectron Spectrometer for elements like carbon, nitrogen, oxygen and fluorine.

For validation of the voriconazole presence in the structure of hydrogel rings, SEM-EDS and UV-lamp (UV Transilluminator) were used. Firstly, samples from groups A and B were preliminary analyzed under UV light since voriconazole show fluorescence as it absorbs the light at 256 ± 1 nm and emits UV light at 372 nm. In case of SEM-EDS, samples from

group A and B were looked under SEM (Cross Beam 540, Carl Zeiss) similarly to the previous method namely two sides of the rings (upper and bottom surface) as well as the inside to determine the presence of fluorine which is present in voriconazole and estimate its relative abundance.

3.3.2. In-vitro drug release

In-vitro experiment on fungi was performed by placing the hydrogels from group A and B into the media containing Aspergillus fungi. The colony of Aspergillus was grown on Petri dish with the help of a research group from Wenzhou Medical University – Eye Hospital. Both hydrogels from groups A and B were incubated in contact with fungi, and the zone of inhibition was recorded.

3.4 Spectrophotometric method for voriconazole determination in drug delivery device

3.4.1. Determination of optical characteristics of voriconazole

For all the below-mentioned experiments, a PhotoLab 7600 UV-VIS spectrophotometer (Xylem Analytics) was used.

Reagents such as phosphate buffer saline (pH=7.4) was prepared by dissolving one tablet in 200 ml of ultrapure water yielding 0.01 M of phosphate buffer solution (0.0027 M of potassium chloride and 0.137 M of sodium chloride). The stock solution of voriconazole, on the other hand, was prepared by weighing 25 mg of pure voriconazole in powder form and dissolving it in a volumetric flask with 25 mL of dimethyl sulfoxide giving the solution with a concentration of 1000 μg/mL. Further standard working aliquots were prepared by taking the stock solution and diluting it with PBS. Aliquots of 1000 μg/mL solution were transferred into thirteen 25 mL vials and volume was adjusted with PBS to give final concentrations of 10, 20, 30, 40, 50, 60, 70, 80, 100, 120, 160, 200 and 240 μg/mL. These series of voriconazole solutions were scanned at 200-400 nm region against PBS blank. The absorbance values for these solutions were noted, and the calibration curve was drawn by plotting concentration values on the x-axis and the absorbance values on the y-axis.

3.4.2. Determination of voriconazole concentration in hydrogel rings

In order to measure the concentration of voriconazole in hydrogel rings and measure the release kinetics, two methods were proposed.

Method 1: Cumulative release of voriconazole

The hydrogel rings from group A were transferred into 7 mL vial containing 1 mL of PBS. Then these vials were placed into the water bath at 37°C to mimic the human body temperature. 1 mL of samples were collected at each time interval points and further diluted with 9 mL of PBS and stored for further analysis. Samples were collected at 10, 20, 30, 40, 50, 60 minutes and then at 2, 3, 4, 5, 6, 12, 24 hours on day 1, then every 24 hours for further five days. The experiments were repeated five times for ring from group A that might show promising results (OD=10 mm, ID=6 mm, H=0.8 mm). In addition, the ring having the same dimensions from group B was used as a true negative control.

Method 2: Release of voriconazole in fresh PBS solutions

The hydrogel rings from group A were transferred into 7 mL vial containing 1 mL of PBS. These vials were placed into the water bath set at a temperature of 37°C, where they maintained for five days. The PBS was collected from the vials at each time points and replaced with fresh PBS. Samples were collected at 6, 12 and 24 hours on day 1, then every 24 hours for a further five days. 1 mL of each sample was diluted with 9 mL of PBS and stored for analysis of voriconazole concentration via a UV-VIS spectrophotometer. The experiments were repeated five times for ring from group A that might show promising results (OD=10 mm, ID=6 mm, H=0.8 mm). In addition, the ring having the same dimensions from group B was used as a true negative control.

Samples for both methods were scanned at 200-400 nm region against PBS blank. The zero-order spectrum for all samples was plotted with recording the absorbance values for the corresponding λ_{max}.

Chapter 4 – Results and Discussion

4.1. Preparation of hydrogel rings

6 Teflon molds were loaded with monomer mixture and placed in a laboratory oven, where they were kept for 15, 20, 30, 40, 50 and 60 minutes. Table 4.1 constructed to determine the optimal time required for the polymerization reaction at 80°C, where m_{ms} is the initial mass of a mold with monomer mixture, and m_f is the final mass of a mold with the polymer in it after the reaction. From there, a theoretical mass of the hydrogel rings (m_{th}) was calculated by subtracting mold mass (m_m) from m_f. As can be seen from Table 4.1, the actual mass of the hydrogel ring in dry form was less than the expected value. This can be explained by the fact that some unreacted reagents and PEG were washed out during the preparation process. The optimal time for hydrogel synthesis was 40 minutes since the rings showed the required mechanical properties, namely, they were transparent and flexible – the two most important features for ocular devices (Figure 4.1). Polymers obtained after 50 and 60 minutes of baking cannot be considered for further experiments as they were highly rigid and brittle. Besides, this experiment showed that 15 minutes is not enough to carry out the polymerization reaction.

Table 4.1. Dependence of hydrogel ring's mass on reaction time

t, min	m_m, g	m_{ms}, g	m_f, g	m_{th}, g	m_h, g
15	26.6368	26.8559	26.8308	0.1940	0
20	26.1896	26.4153	26.3885	0.1989	0.0421
30	26.7165	26.8871	26.8495	0.1330	0.0588
40	26.6423	26.8289	26.7744	0.1321	0.0760
50	26.9783	27.1873	27.1290	0.1507	0.0923
60	26.7634	26.9193	26.8606	0.0972	0.0618

Note: m_m = mass of the mold

m_{ms} = mass of the mold filled with monomer solution (before heating)

m_f = mass of the mold filled with monomer solution (after heating)

m_{th} = theoretical mass of the hydrogel rings

m_h = actual mass of the hydrogel rings (after washings and drying)

Figure 4.1 demonstrates the hydrogel rings obtained after NVP polymerization. Initially, hydrogels were transparent. However, after they were placed into the water, the transparent parts become opaque. This happens due to the fact that PEG, which was initially present in the structure of the hydrogel, exchanged with water molecules during the washing procedure. The same explanation can be found in the study performed by Bartolo [58], where they synthesized hydrogel from cyanoethyl acrylate, PEG 300 and PEG-DA in 9:10:1 ratio. The opacity of this device might create some difficulties during the clinical testing on a human model as it would interfere with the vision of the patient.

Regarding the size of the rings, the hydrogels were equally sized before washing with water, namely had the following dimensions: OD = 10 mm, ID = 6 mm and H = 0.8 mm. After 30 minutes in water, the size did not change. However, after immersion of hydrogel rings in water for 24 hours, the diameter was slightly increased by approximately 0.5 - 1 mm (Figure 4.1, B). This observation can be explained by the fact that hydrogels have a favorable property to swell in the presence of a thermodynamically compatible solvent, in this case – water.

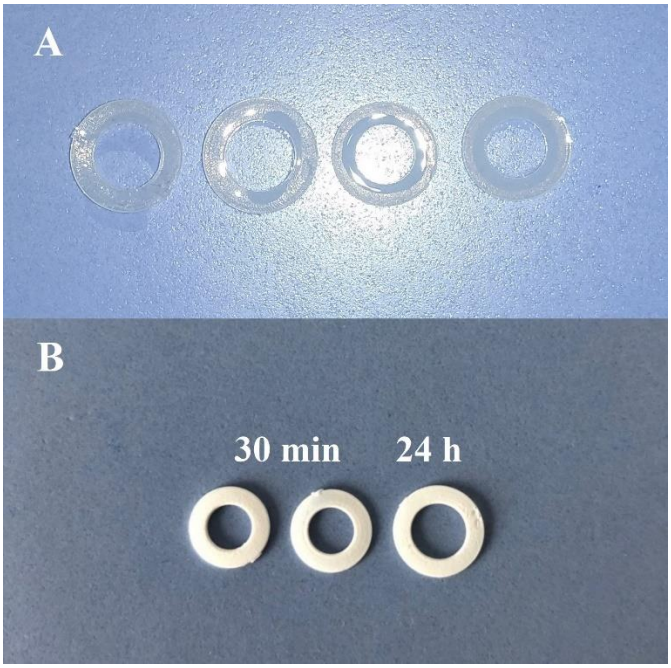

Figure 4.1. Hydrogel rings with various diameter and height: before (A) and after (B) contact with water. **Note:** After 24 hours in the water, the diameter was slightly increased by approximately 0.5 - 1 mm (B)

4.2. Morphological analysis

4.2.1. Surface characterization: X-Ray Photoelectron Spectroscopy

XPS technique was used to analyze the surface chemistry of hydrogel rings by measuring the elemental composition and chemical state of our synthesized polymer. The material may consist of several layers; therefore, the chemical and physical properties of the topmost surface layer can differ from bulk material. XPS analysis of hydrogel rings that did not contain voriconazole in it showed three distinct peaks representing the presence of carbon, hydrogen and oxygen (Figure 4.6). According to Figure 4.4. the highest intensity in the C1s region was observed at 284 eV. C1s spectrum typically contains four main components, namely C-C, C-H, C-O and C=O, and each component tend to have a symmetric peak. The peak observed at 284 eV represents the C-C and C-H in the hydrogel structure. However, it should be noted that this peak is slightly shifted to the right due to the presence of another peak (C=O component) at 288 eV. Other peaks found at 398 and 531 eV represent N1s (N-C) and O1s (O=C) chemical state, respectively. Figure 4.2 demonstrates that PVP has C-C, C-H, C=O and C-N bonds, which means that the above stated XPS analysis data verify that our synthesized hydrogel rings indeed consist of PVP.

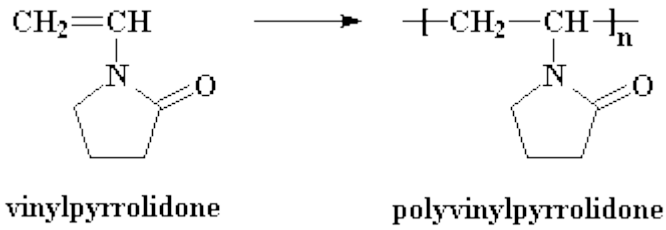

Figure 4.2. Polymerization of vinylpyrrolidone

The same results can be observed in the analysis of hydrogel rings containing voriconazole (Figure 4.4 and 4.5). However, in this case, the XPS analysis reveals an additional peak that was found at 686 eV (Figure 4.5). This means that organic fluorine (C-F) is present on the surface of the hydrogel. Since voriconazole contains C-F components in its structure (Figure 4.3), it can be concluded that the procedure of loading the drug into the hydrogel structure was successful.

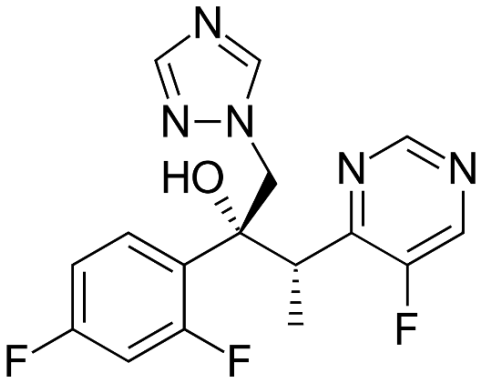

Figure 4.3. Chemical structure of voriconazole

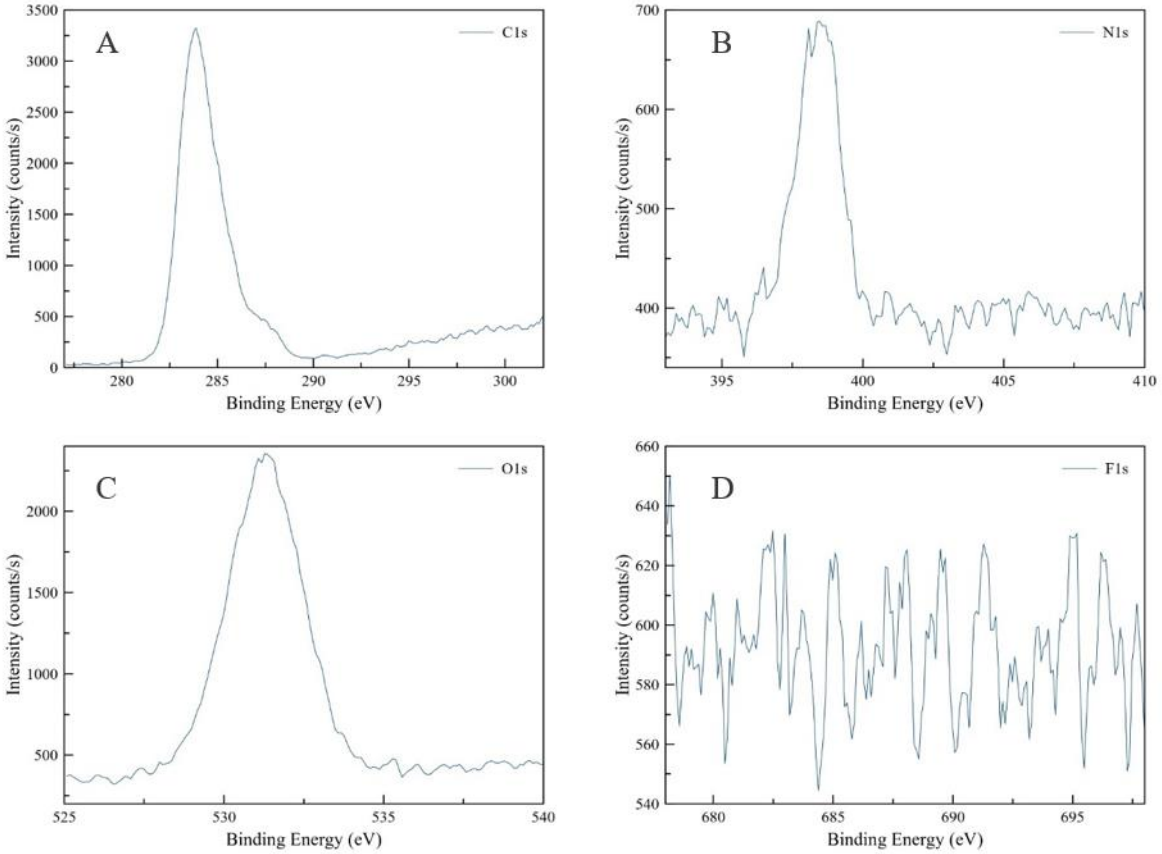

Figure 4.4. XPS spectra of hydrogel rings without voriconazole (group B).

Note: (A) C1s: peaks found at 284 and 288 eV represents the C-C, C-H and C=O bonds in the hydrogel structure, respectively. (B) N1s: peak at 398 eV demonstrates the C-N bond. (C) O1s: peak at 531 eV demonstrates the C=O bond. (D) F1s: no peaks were found.

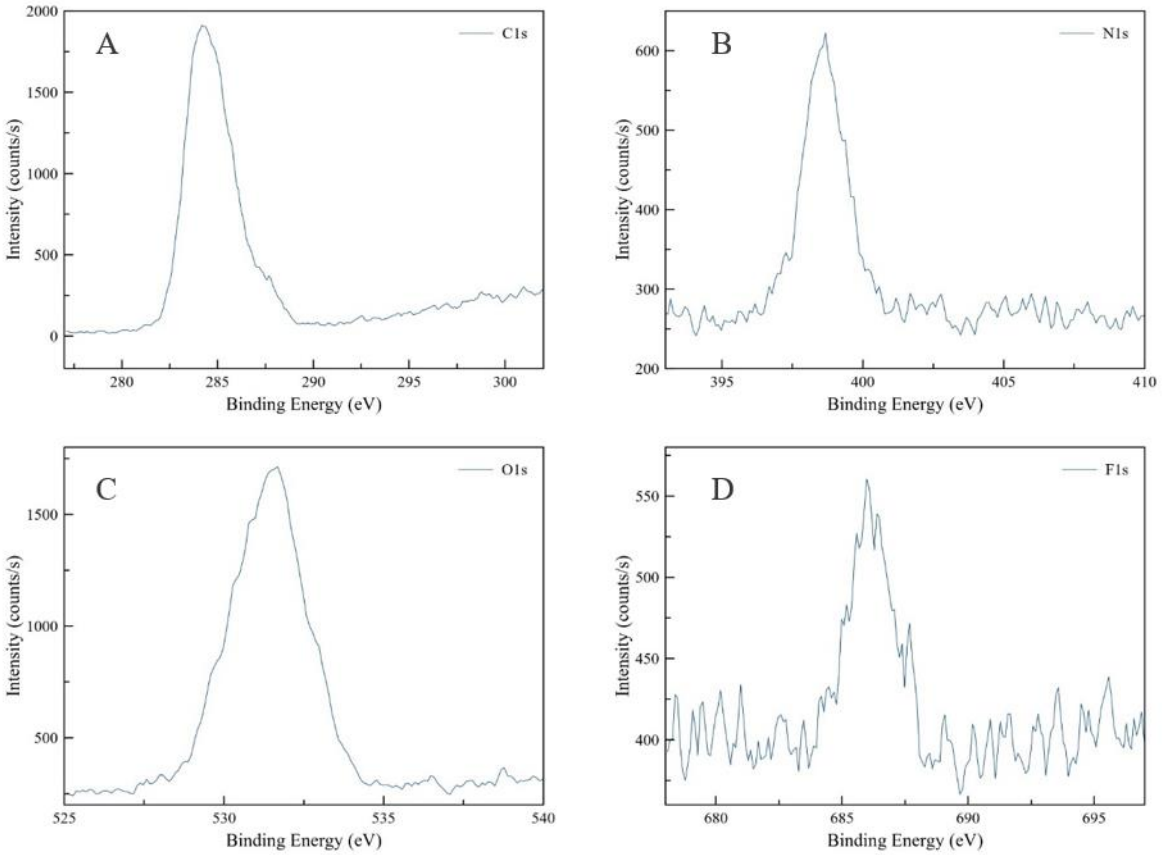

Figure 4.5. XPS spectra of hydrogel rings with loaded voriconazole (group A)

Note: (A) C1s: peaks found at 284 and 288 eV represents the C-C, C-H and C=O bonds in the hydrogel structure, respectively. (B) N1s: peak at 398 eV demonstrates the C-N bond. (C) O1s: peak at 531 eV demonstrates the C=O bond. (D) F1s: the peak detected at 686 eV represents the C-F bond, which is a component in the structure of voriconazole.

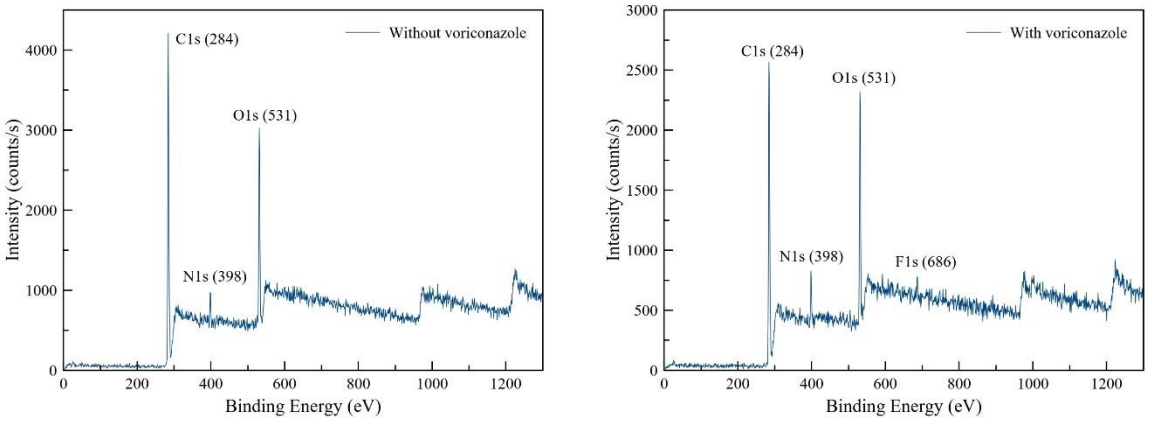

Figure 4.6. XPS spectra of hydrogel rings: without voriconazole (left) and with voriconazole (right)

4.2.2. Surface characterization: Scanning Electron Microscopy

The hydrogel rings have two surfaces (top and bottom) with different morphological structures since they were exposed to the different environments during polymerization reaction: the top surface was exposed to ambient air and the bottom surface was in contact with Teflon surface (Figure 4.7). Therefore, as it was prescribed in the methodology part, the top and bottom surface of hydrogels were analyzed by SEM for both groups. SEM images demonstrated that the process of washing out PEG was completed successfully, as pore structure was observed in all polymers from groups A and B. Therefore, synthesized polymers have the ability to absorb a certain amount of drug and release it when need it.

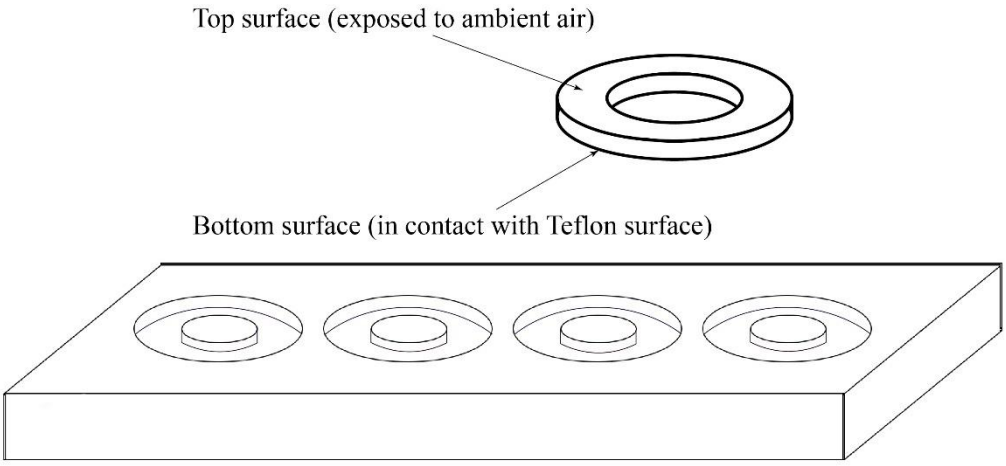

Figure 4.7. Schematic representation of hydrogel ring

Figure 4.8 and 4.9 reveals the porosity and nature of the hydrogel structure. From both figures, it can be stated that the morphology of the top and bottom surface of hydrogels is slightly different in terms of its pore size and volume. For example, the top surface of hydrogel was in contact with the atmosphere, whereas the bottom part was in contact with Teflon mold. Due to this fact, the bottom surface was flattened, and the upper surface was able to have a porous structure. This observation is indeed crucial in clinical application since it is important to know from what side of the hydrogel ring the drug release will occur. Therefore, the top surface of the hydrogel ring should be placed in the eye surface as only from there, the drug can be released more efficiently.

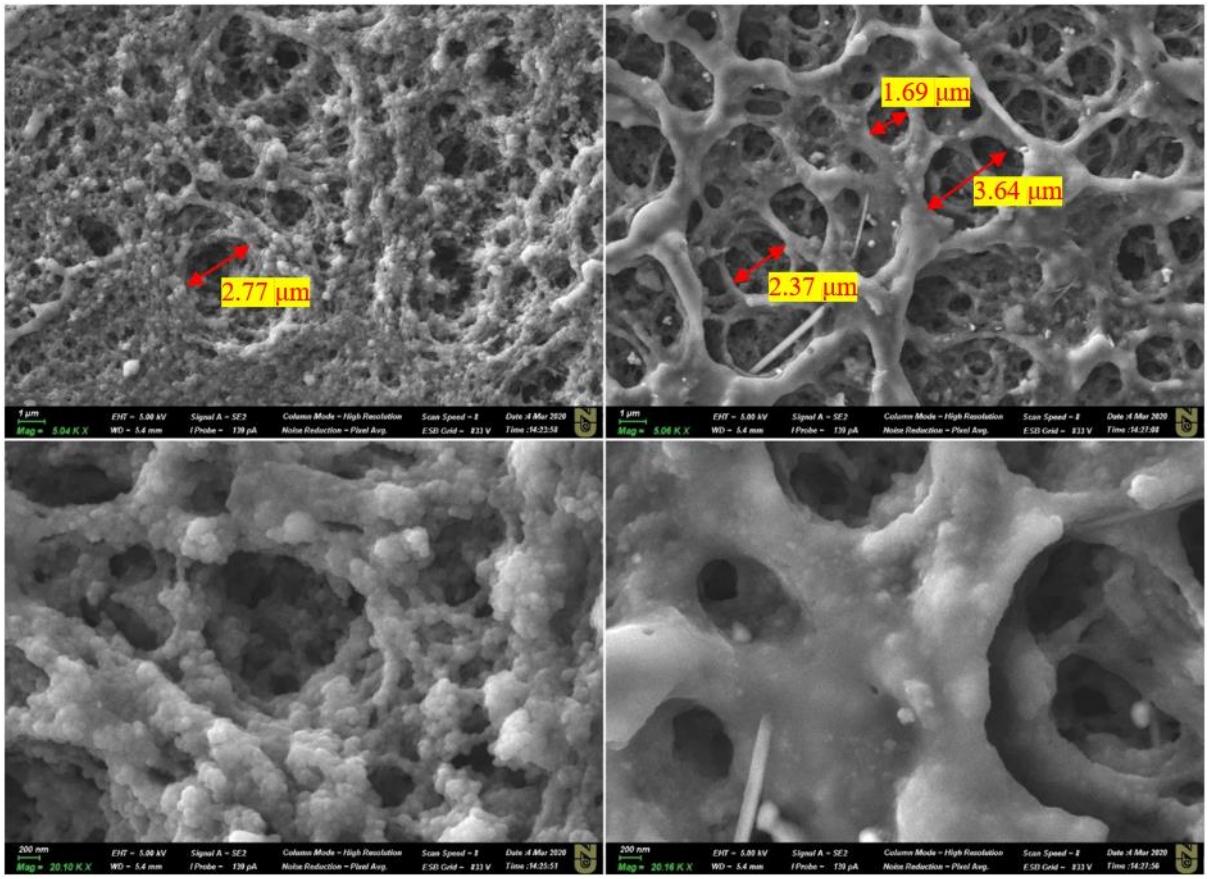

Figure 4.8. SEM images of hydrogel rings without voriconazole loading: bottom surface (left column) and the top surface (right column) at x5K and x20K magnification

Comparing these two SEM images, the solid crystals of voriconazole was only found in Figure 4.9.

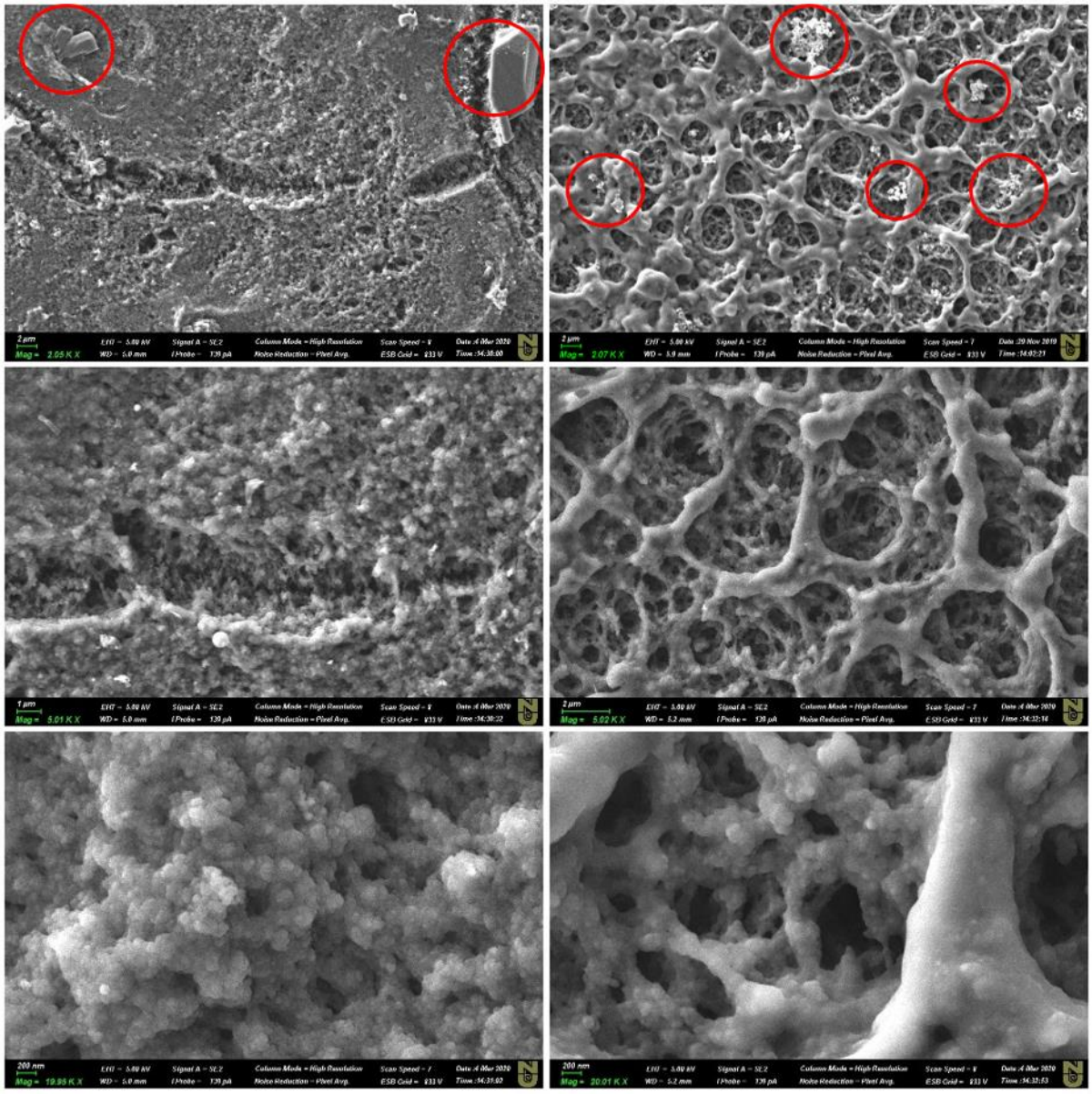

Figure 4.9. SEM images of hydrogel rings with voriconazole loading: bottom surface (left column) and the top surface (right column) at x2K, x5K and x20K magnification. **Note:** Red circles represent the deposition of voriconazole crystals on the hydrogel matrix.

4.2.3. Pore size distribution: Mercury porosimetry analysis

The presence of pores in the material of the polymer rings was verified by SEM; however, this technique cannot give quantitative measurements of the degree of porosity and the size of the pores. For this purpose, mercury porosimeter was used to identify the pore diameters as well as its volume. The results were summarized in Figure 4.10, where a hydrogel ring sample from group B with a mass of 0.0491 g and a volume of 0.0402 cm^3 (OD = 10 mm,

ID = 6 mm, H = 0.8 mm) was examined. Figure 4.10 reveals that half of the pore volume (54%) was occupied by pores having a diameter from 5 to 25 nm, whereas the other half (46%) have pores in the range of 7-240 μm.

The porosity can be calculated through this formula: $\phi = \frac{Vv}{Vt}$, where V_v is the volume of void space and V_t is the total volume of a hydrogel. In addition, using Figure 4.10, the void volume was calculated by summing up the normalized volumes at a corresponding pore diameter. The total specific volume of the pores was 0.2478 cm^3/g.

$V_t = \pi \times (R_{OD} - R_{ID})^2 \times H = \pi \times (1 - 0.6)^2 \times 0.08 = 0.0402\ cm^3$

Therefore, the porosity of hydrogel rings, $\phi = \frac{0.2478\frac{cc}{g} * 0.0491g}{0.0402\ cc} = 0.30$

Considering the fact that the average volume of eye drops is equal to 0.05 mL [58], then these hydrogel rings can intake up to 0.012 mL. This value is sufficient, since these rings will be loaded with a crystalline drug, and a porosity of 30% will provide enough space for penetration and precipitation of voriconazole crystals in the pores of the polymer rings.

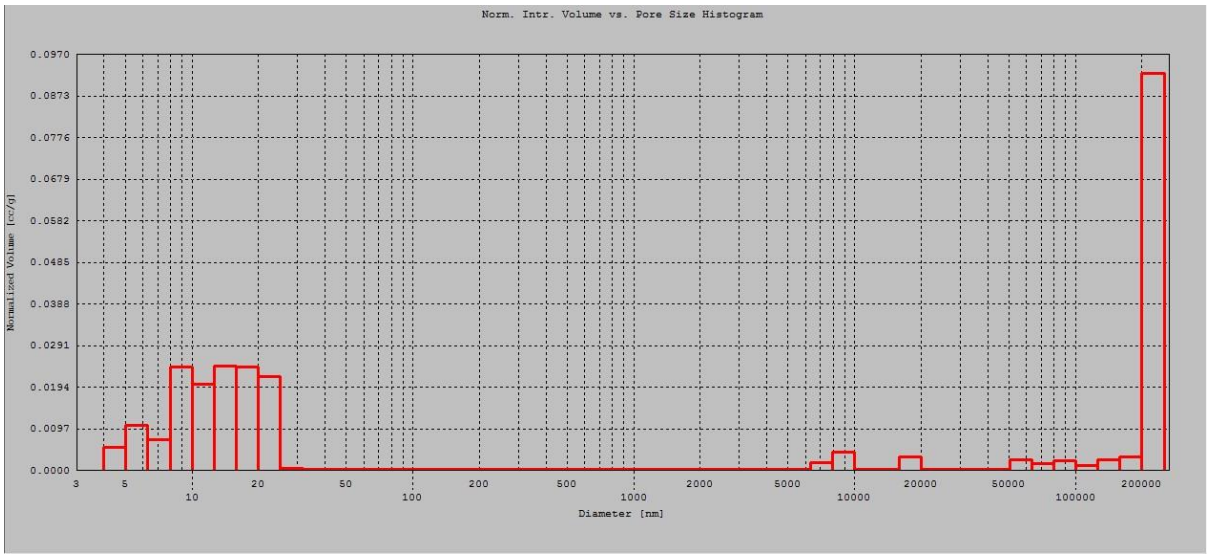

Figure 4.10. Mercury porosimetry analysis of hydrogel rings

4.3. Determination the presence of voriconazole in hydrogel rings

The simplest method of validation of the presence of voriconazole is placing it under the UV-lamp. Figure 4.3 allows us to predict that voriconazole will be fluorescent under UV light as it has double bonds (conjugated bonds), which enable it to absorb the light in the UV-region and emit the energy in the form of a glow. Figure 4.11 confirms this statement as the

hydrogel ring loaded with voriconazole glowed compared to the polymer that does not have this drug in the formulation. Voriconazole absorbs light at approximately 256 nm (UV), and emits light at 372 nm, therefore, the right ring in Figure 4.11 has violet/bluish color. In the case of hydrogel ring from group B, which was not loaded with voriconazole, it shows no fluorescence under UV-light.

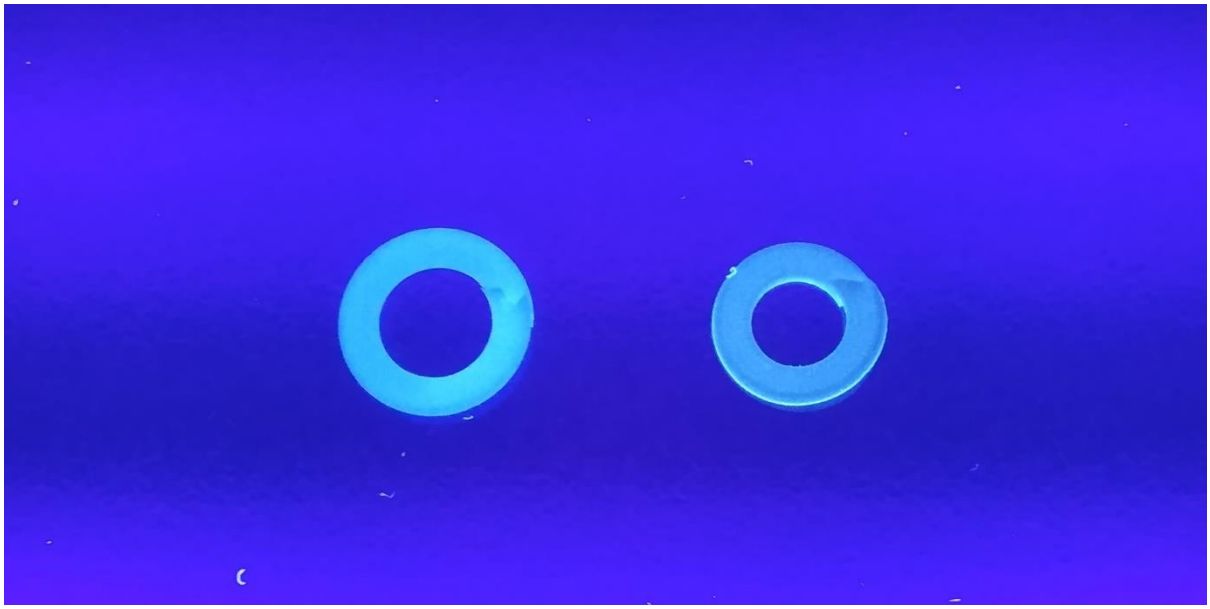

Figure 4.11. The hydrogel rings under UV light: group A (left ring) and group B (right ring)

Note: group A = “drug-loaded”, group B = “unloaded” hydrogel rings

Another qualitative measurement of voriconazole was done by analyzing samples from groups A and B using energy-dispersive X-ray spectroscopy (SEM-EDS). This technique allows determining the presence of chemical elements as well as their relative abundance in a sample. Thus, in combination with any SEM images, EDS is useful to obtain an elemental analysis of the interested area. Compared to XPS, EDS has a technique to inspect the “exact” position of the chemical elements on the image obtained from SEM. In these studies, the relative abundance of carbon, oxygen and fluorine were investigated (Figure 4.12 - 4.15). As it was earlier stated, our synthesized polymer rings have two sides that have different porosity level. Therefore, samples from groups A and B were looked under SEM to determine the presence of fluorine and estimate its relative abundance. Since the chemical structure of voriconazole consists of carbon, hydrogen and fluorine atoms, the latter indicates the presence of the drug on SEM-EDS image. Figures 4.12 and 4.13 demonstrate the EDS analysis of the top and bottom surface of the hydrogel ring, which was loaded with voriconazole (group A). The regions that have red, green and pink color illustrate the presence of fluorine, oxygen and

carbon atoms in the hydrogel matrix, respectively. From these two images, it can be concluded that a higher concentration of fluorine was found on the top surface of a hydrogel ring (14.1 wt.%) compared to the bottom surface that contained 3.3 wt.%. This observation suggests that the top side of the ring has a property to adsorb more voriconazole crystals than the bottom side due to the highly porous structure of the polymer matrix.

Figures 4.14 and 4.15 demonstrate the analysis of hydrogel ring from group B (control group), which did not contact with voriconazole. As expected, no traces of fluorine were found in the EDS spectrum.

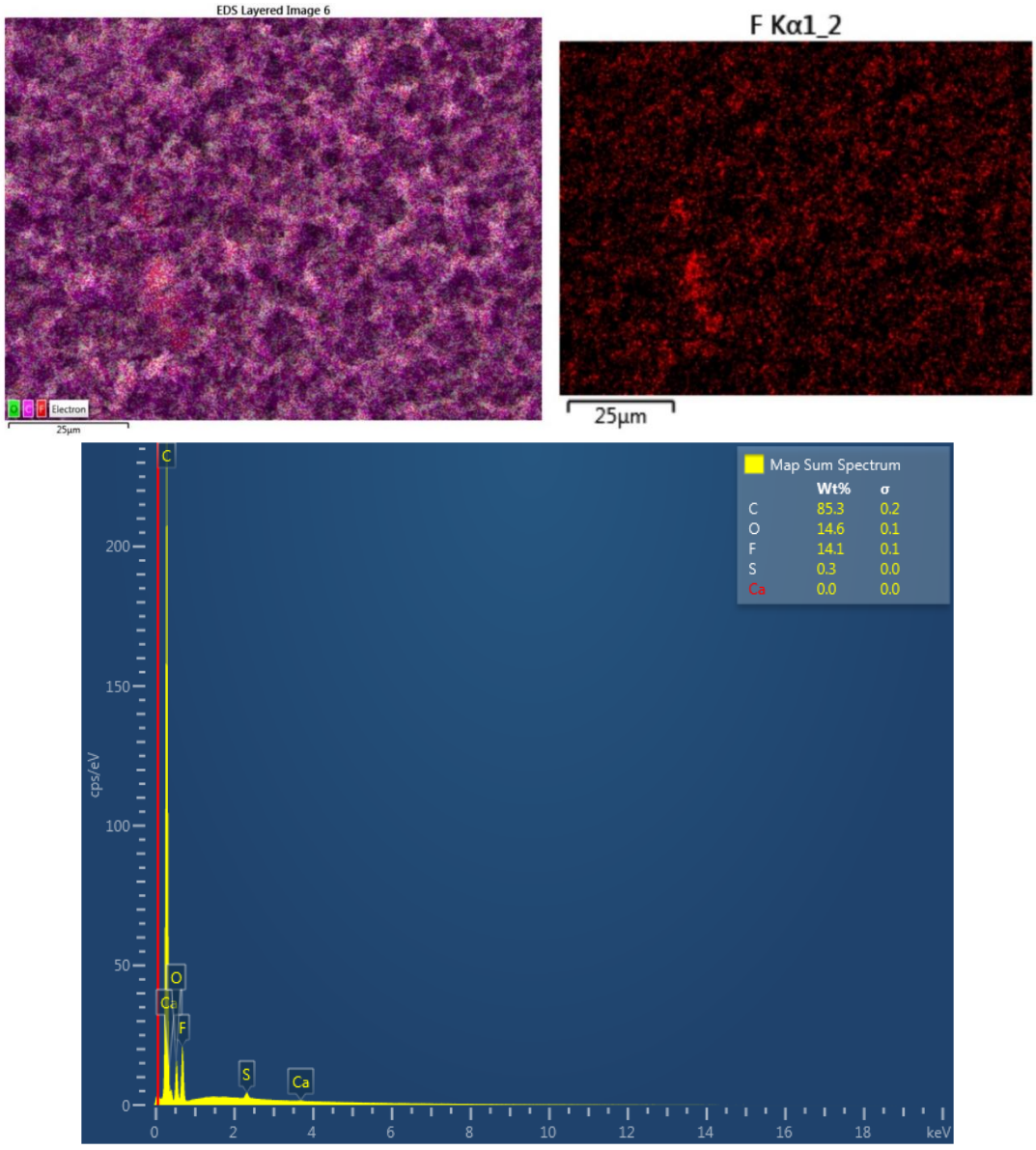

Figure 4.12. EDS mapping of SEM analysis of "drug-loaded" hydrogel ring (top surface). **Note:** The regions that have red, green and pink color illustrate the presence of fluorine, oxygen and carbon atoms in the hydrogel matrix, respectively.

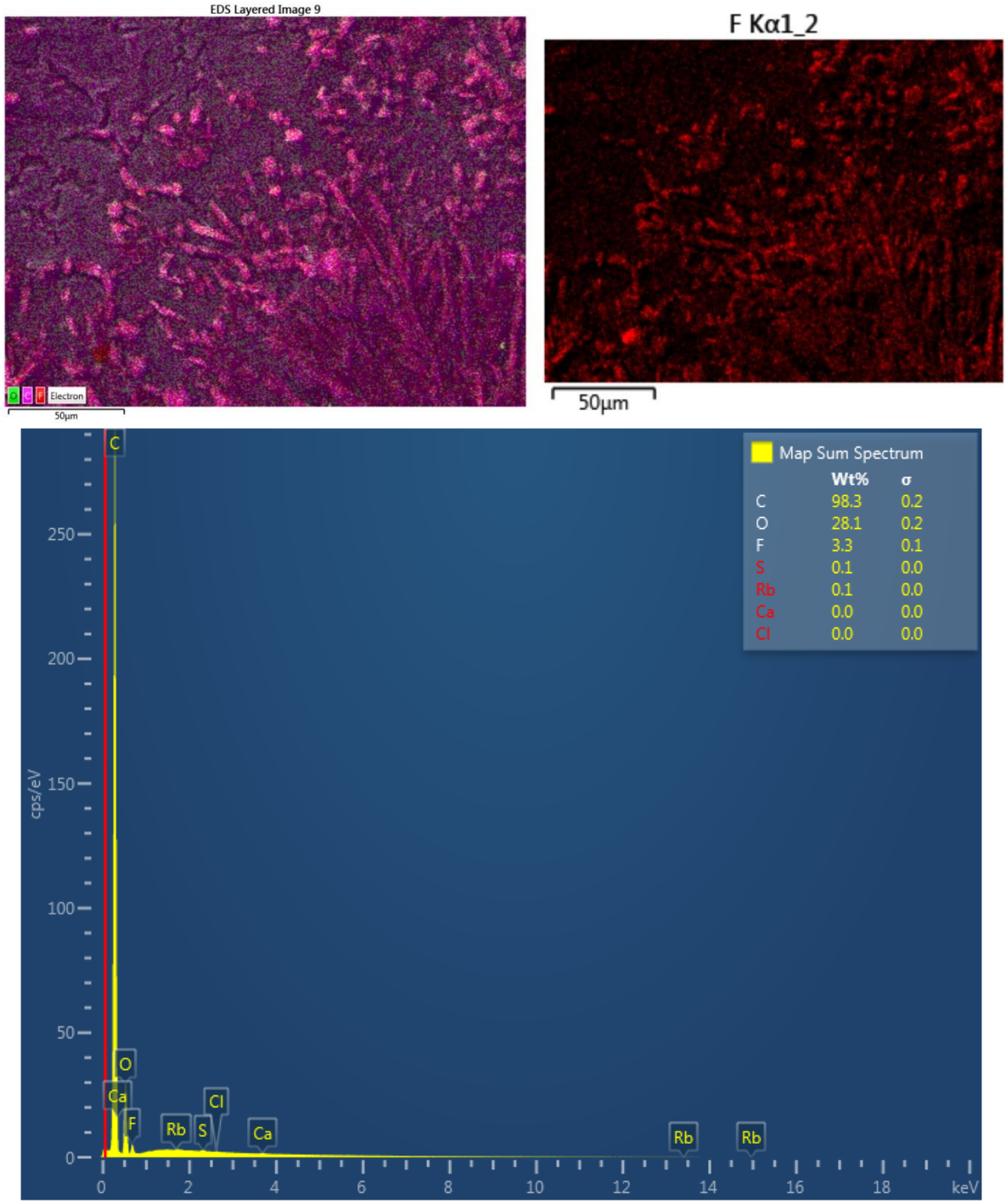

Figure 4.13. EDS mapping of SEM analysis of "drug-loaded" hydrogel ring (bottom surface).

Note: The regions that have red, green and pink color illustrate the presence of fluorine, oxygen and carbon atoms in the hydrogel matrix, respectively.

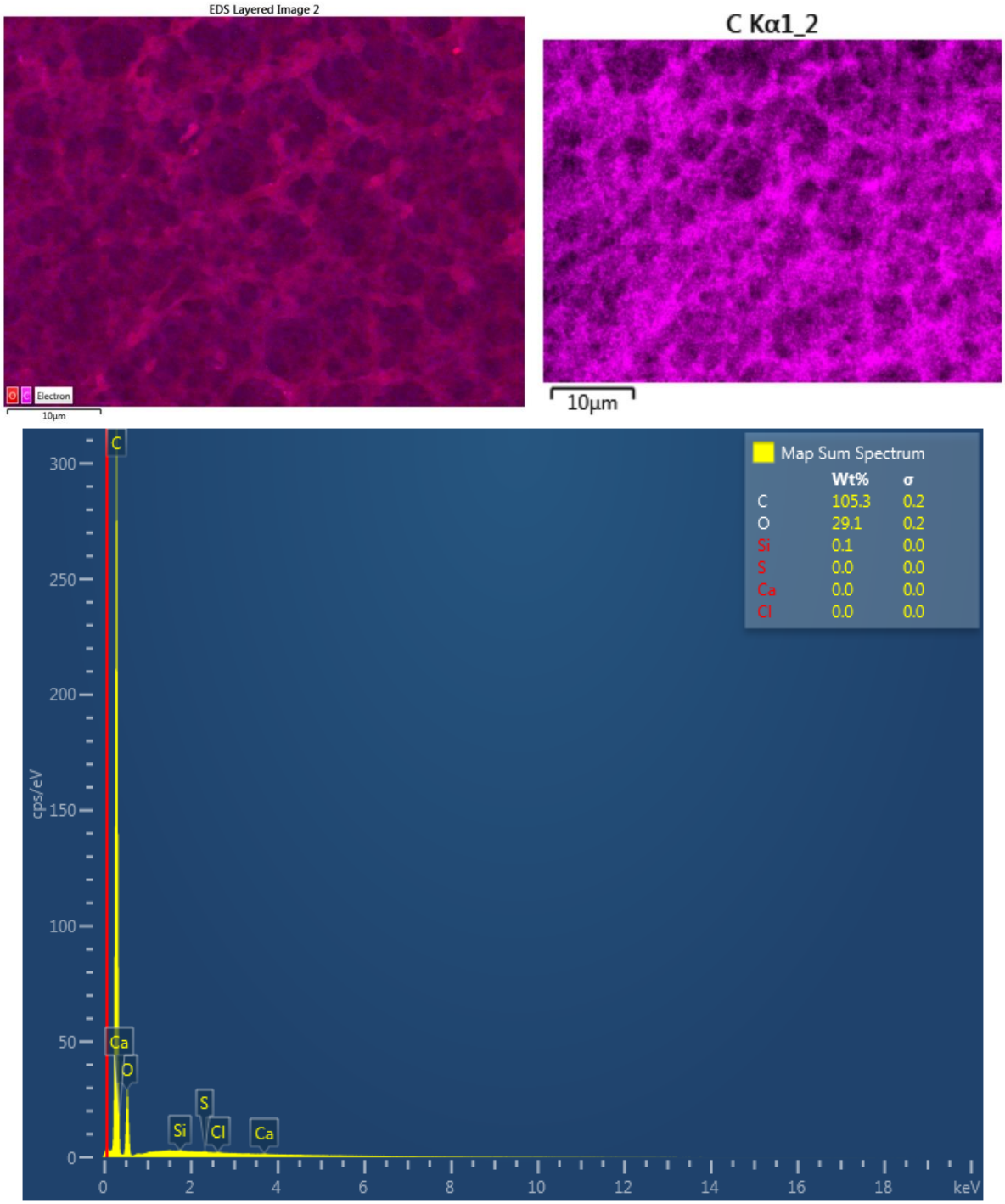

Figure 4.14. EDS mapping of SEM analysis of "unloaded" hydrogel ring (top side). **Note:** The regions that have red and pink color illustrate the presence of oxygen and carbon atoms in the hydrogel matrix, respectively.

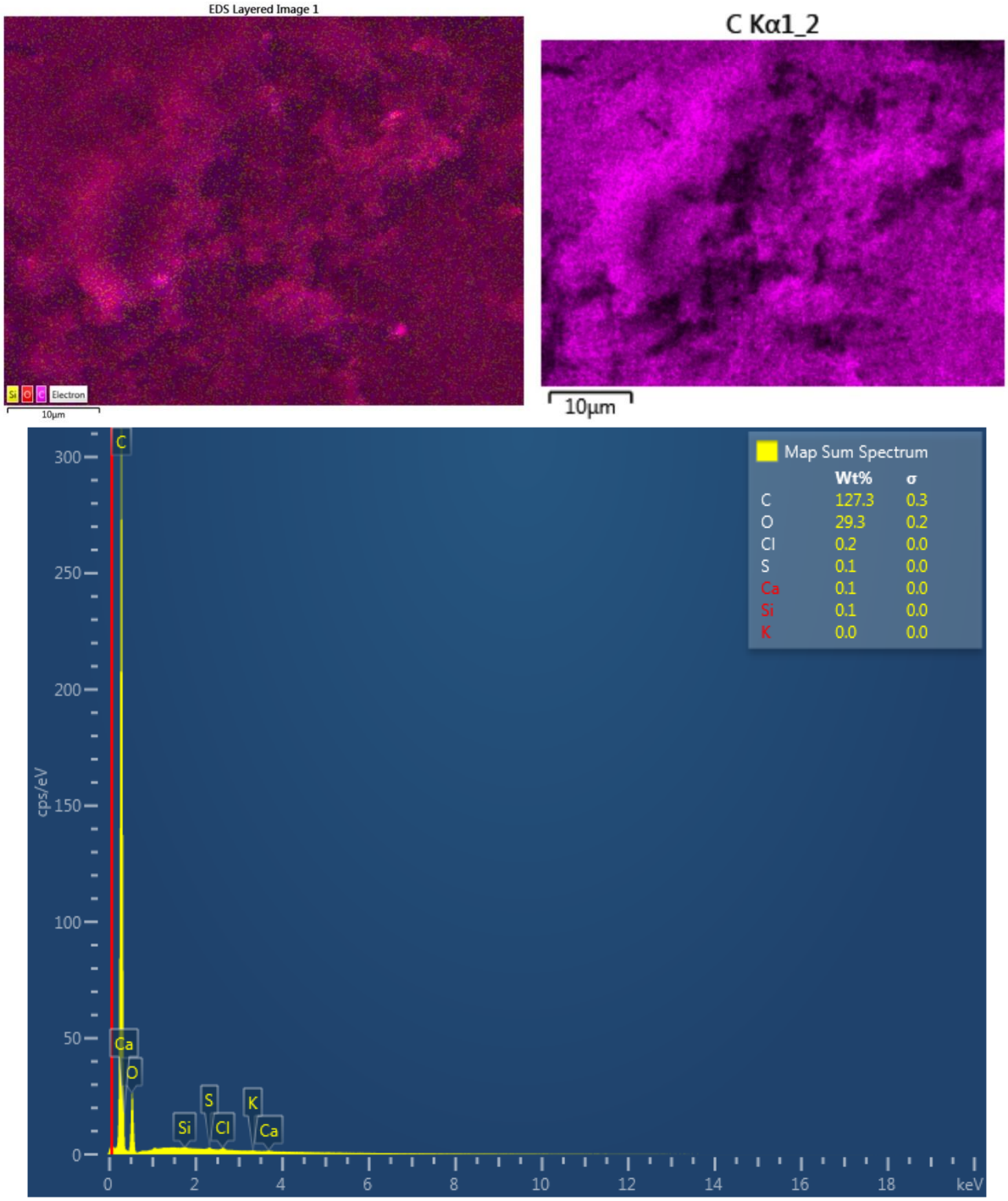

Figure 4.15. EDS mapping of SEM analysis of "unloaded" hydrogel ring (bottom side). **Note:** The regions that have red and pink color illustrate the presence of oxygen and carbon atoms in the hydrogel matrix, respectively.

4.4. In-vitro drug release

In these experiments, fungi, which are *clinical isolates,* were used. This means that the fungi were first biopted from an infected patient, and cultured *in vitro* and stored subsequently. Experiments were performed with the fungus *Aspergillus* and *Fusarium.* These filamentous fungi were chosen since they are major causes of corneal diseases (fungal keratitis) worldwide, leading to severe visual impairment and, in worst cases, blindness. The plasma membrane of *Aspergillus* and *Fusarium* is similar to a plasma membrane that mammals have with one difference: nonpolar ergosterol acts as a principal sterol in fungi, whereas in mammals, this function is replaced by cholesterol. Voriconazole inhibits ergosterol biosynthesis, which in turn affects the plasma membrane formation. As the membrane permeability changes, the growth of fungi would be inhibited [9, 21].

It is important to mention that instead of the rings, the hydrogel rods were used in this experiment. The chemical composition of rods is identical to the rings, the only difference is the shape. Fungi were spread over the entire surface of a Petri dish. Then a rod of group A (loaded with voriconazole) and a rod of group B (unloaded control) were placed on the disc's surface. The Petri dishes were incubated at 37°C for several days and then inspected and photographed. Figure 4.16 (left) shows the Petri dish after 2 days of incubation at 37^{o}C. Clearly, no living *Aspergillus* is present around the drug-loaded rod, whereas undisturbed growth and development of the fungus is seen around the unloaded control rod. The empty region around the drug-loaded rod is a so-called "zone of inhibition". The fungus was killed there, as a result of voriconazole diffusing away from the drug-loaded rod (slow movement of the drug against concentration gradient). Therefore, the concentration of voriconazole decreases gradually upon going from the rod's surface toward the edge of the zone of inhibition. At the periphery of the zone, the concentration is just low enough to allow the neighboring fungi to survive (this is the so-called "minimal inhibitory concentration"). There are three independent observations to support the idea of diffusion-controlled drug release. One is the observation that the zone of inhibition is elliptical, which is expected since the drug-releasing device is rod-shaped. The second observation is that the zone of inhibition expanded with time; this was especially clear during the first 2 days. The third is the observation that identical hydrogel materials but with elevated porosity (obtained by using more polyethylene glycol in the monomer formulation, vide supra) produced a larger zone of inhibition at the same time of observation. A clear illustration of the second point is provided in Figure 4.16 (right). Here, the material has elevated porosity as 20 % PEG was used in the formulation (rather than 10 %); the difference in the size

of the zones of inhibition is clear during the comparison of the left and right images in Figures 4.16.

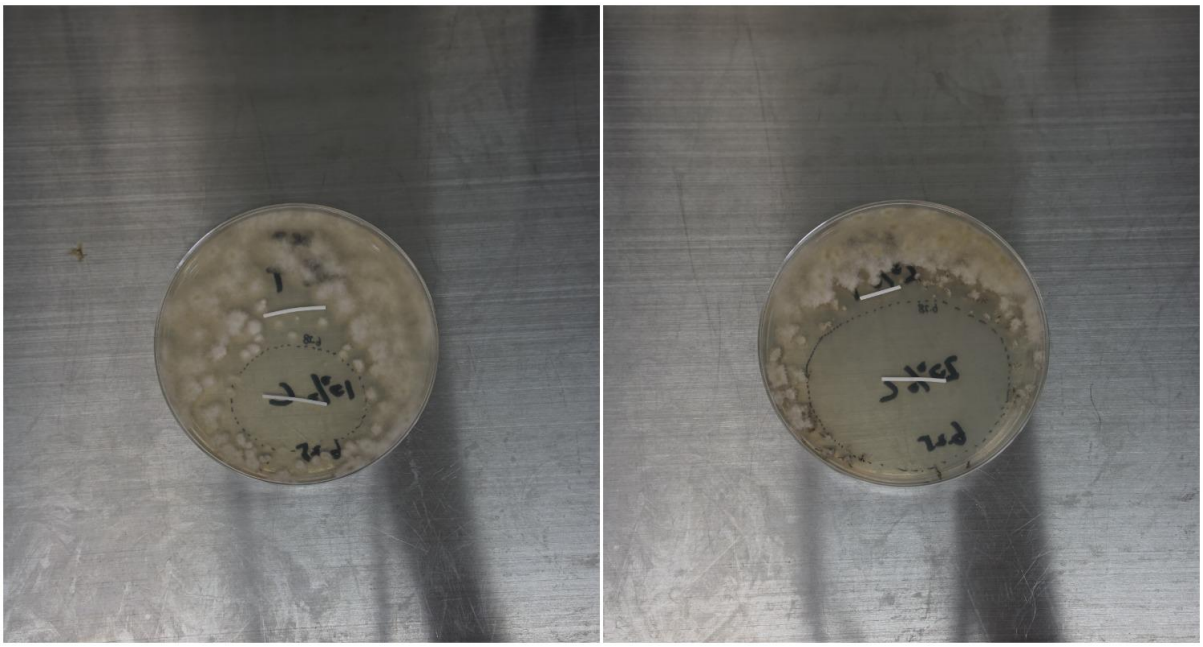

Figure 4.16. In vitro test on *Aspergillus*: 10 wt.% PEG (left) and 20 wt.% PEG (right)

4.5. Load and release rate

4.5.1. Determination of optical characteristics UV extinction of voriconazole

Thirteen samples of voriconazole of known concentration were analyzed and the corresponding spectra were plotted and summarized in Figure 4.17. It can be clearly seen in Figure 14.7 (A) that the maximum absorbance was observed at 256 nm for all eight voriconazole samples. However, the peaks are shifted towards the higher wavelength as the concentration increased from a certain point, namely after 100 μg/mL (Figure 14.7 (B)). In addition, after 80 μg/mL, the linearity disappears, so that the absorbance values did not change as the concentration of voriconazole was increased. This phenomenon can be observed due to the limitation of Beer-Lambert's law. Therefore, for the calibration curve, the concentration region from 10-80 μg/mL was selected as it obeys Beer's law.

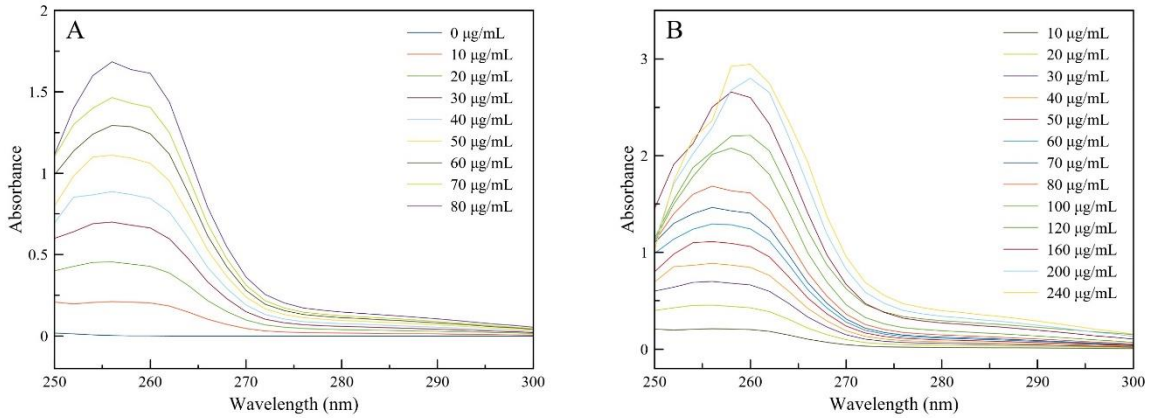

Figure 4.17. UV absorption spectra of voriconazole

Table 4.2 was constructed to compare our results with previously published methods. It can be stated that the method described in this work correlates with other papers, namely, the wavelength at maximum absorbance is the same (256 nm) and the linearity exists within the range of 10-80 μg/mL.

Table 4.2. Comparison of spectrophotometric results with the current method

Solvent	λ_{max}, nm	Linearity, μg/mL	Reference
Water	252	5-80	[59]
HCl	256	10-60	[60]
Methanol	256	5-30	[61]
PBS (pH 7.0)	256	5-60	[62]
PBS (pH 7.4)	256	10-80	Present method

The concentration values, as well as their corresponding absorbance, were plotted to find out all necessary parameters required for the identification of the voriconazole concentration in the hydrogel rings (Figure 4.18).

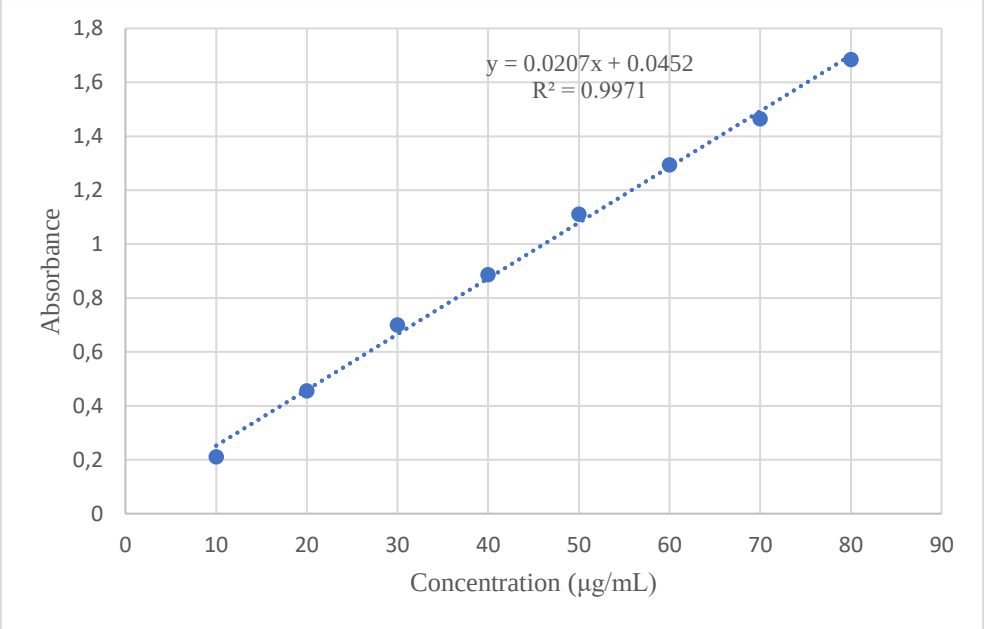

Figure 4.18. Calibration curve of voriconazole solutions

Table 4.3. Optical characteristics of voriconazole

Parameter	Current method
λ_{max}, nm	256
Linearity, µg/mL	10-80
Slope	0.0207
Intercept	0.0452
Correlation coefficient	0.9971

4.5.2. Determination of voriconazole concentration in hydrogel rings

Using Table 4.3, the voriconazole quantity that escaped from the rings was measured for two methods. Firstly, the determination of the cumulative release of the drug was based on measuring the absorbance values at 256 nm for five days and putting these values into the equation from Figure 4.18. To monitor the drug release, the hydrogel rings (OD=10 mm, ID=6 mm, H=0.8 mm) from group A were transferred into 7 mL vial containing 1 mL of PBS. Then these vials were placed into the water bath at 37°C to mimic the human body temperature. 1 mL of samples were collected at each time interval points and further diluted with 9 mL of PBS. Dilution was required since a high concentration of voriconazole cannot be detected with UV-Vis spectrophotometer. Recorded absorbance values were put into the following equation: A = 0.0207x + 0.0452, where A is the absorbance at the selected time point and x is a

corresponding concentration value. The obtained results were summarized in Figure 4.19, where voriconazole was released from the hydrogel ring in a sustained manner for 2 days. After 2 days the concentration of voriconazole in 10 mL of PBS solution was not significantly changed, showing the value of 80 μg/mL.

Another performed release study was illustrated in Figure 4.20, where hydrogel rings were subjected to a new PBS solution environment refreshment. The procedure is similar to the previous method, namely the hydrogel rings ((OD=10 mm, ID=6 mm, H=0.8 mm) from group A were transferred into 22 mL vial containing 10 mL of PBS. These vials were placed into the water bath set at a temperature of 37°C, where they maintained for 10 days. The PBS was collected from the vials at each time points and replaced with fresh PBS. Figure 4.20 demonstrates that the voriconazole present in the device was almost totally released at day 10. Another observation that can be made from Figures 4.19 and 4.20 is that drug released by simple diffusion, where the diffusion mechanism itself is controlled by the polymeric network of hydrogel ring and limited by the solubility of the drug in PBS.

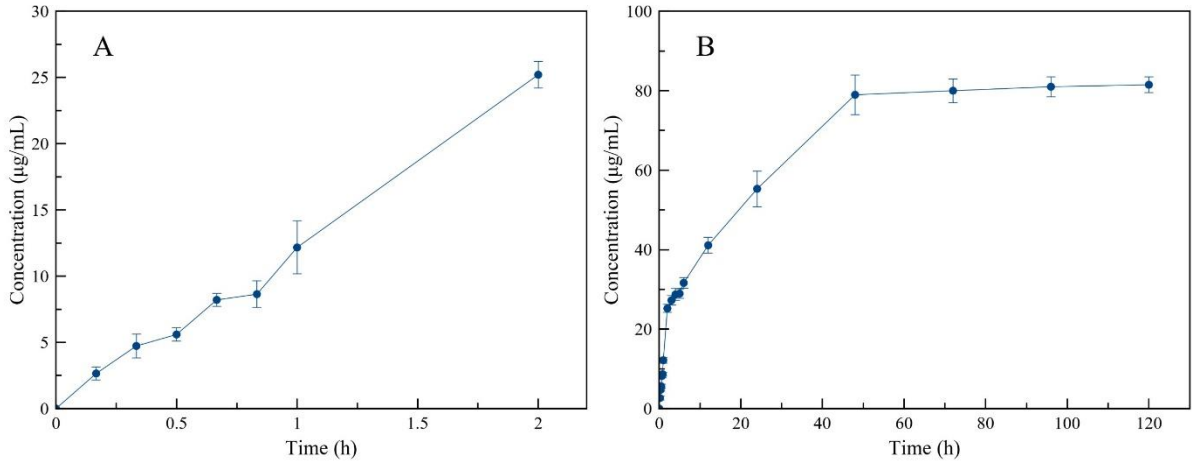

Figure 4.19. Cumulative release of voriconazole from the hydrogel ring (OD=10 mm, ID=6 mm, H=0.8 mm) for 2 hours (A) and 5 days (B)

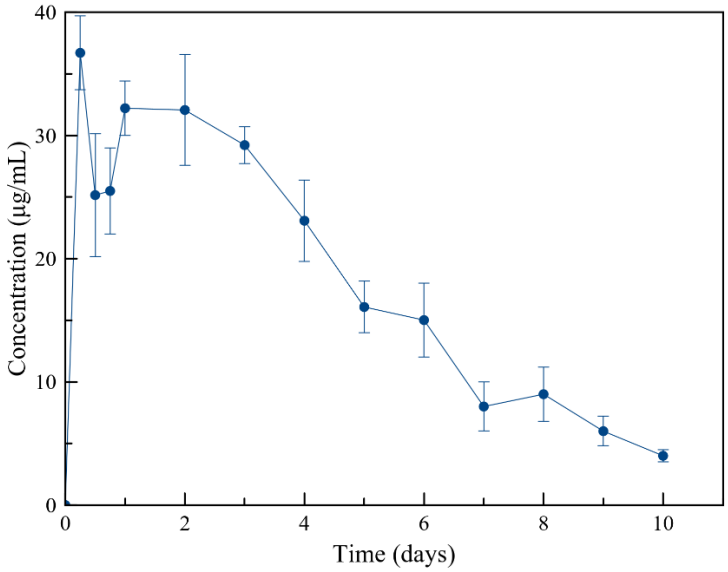

Figure 4.20. Release of voriconazole from the hydrogel ring (OD=10 mm, ID=6 mm, H=0.8 mm) for 10 days

The amount of voriconazole present in ophthalmic eye drops and hydrogel rings can be compared. For example, the ophthalmic solution for eye drops contains 1% voriconazole solution (10 mg/mL) [21]. Considering the fact that the volume of one eye drop is 0.05 mL, then the amount of voriconazole is 500 μg. If the volume of the PBS solution was 10 mL, then the amount of voriconazole that was released from 1 ring during 2 h is 250 μg (10 mL x 25 μg/mL) and after 2 days is 800 μg (10 mL x 80 μg/mL). So, the drug-loaded ring will bring approximately 800 μg of the drug to the ocular surface, whereas an eye drop brings approximately 500 μg of the drug to the ocular surface. Thus, the ratio (drug from ring) : (drug from eye drop) = 1.6 : 1.

For eye drops, it is known that the drug rapidly disappears from the ocular surface. There is a short concentration peak, leading to the high bioavailability of the drug, followed by a rapid decay in concentration, which is associated with limited (to none) bioavailability. Approximately 90% of the drug is spilled.

For the circular device, the release of the drug is occurring for two days. This indicates longer (so: better) bioavailability. Drug molecules releasing from the outer surface and the outside-facing surface may be removed by lacrimal drainage. So, there will be a loss of the drug as well. Drug molecules releasing from the epithelium-touching surface and the inner ring surface will be able to diffuse toward the site of the infection, this inducing a therapeutic effect. Thus, it can be stated that the hydrogel ring can replace one drop of voriconazole solution in

the form of ophthalmic eye drops. It should be noted that this method of studying the release kinetics of voriconazole is not ideal. As was previously mentioned by Bajgrowicz et al. [44] using this method, the hydrogel rings are exposed to a large volume of PBS solution compared to human tear fluid. Thus, the drug can escape the device in a short period as it is released by a simple diffusion mechanism. Drug-distribution, bioavailability and therapeutic efficacy are hard to predict at this stage. This must be evaluated experimentally, both *in vitro* and (with animal) models *in vivo.*

Chapter 5 - Conclusion

This work presents the concept of creating a drug delivery device in the form of hydrogel rings that has the potential of treating fungal keratitis effectively. The main objective of this work was to show that a particular drug delivery device can provide drug concentration at a therapeutic level for a long duration, excluding the frequent application of the eye drops. XPS and SEM-EDS analysis demonstrated that our synthesized hydrogel rings indeed consist of PVP, and voriconazole loading into the hydrogel structure was successful. In addition, the porosimetry test verified that hydrogel rings have pores with diameters 5-25 nm (54%) and 7-240 μm (46%), and a porosity of 30% provides enough space for penetration and precipitation. In vitro release studies demonstrated that the drug of choice – voriconazole was released from our device and inhibited the fungal growth. Moreover, the drug release experiments showed that voriconazole released from the device during the two days, and after the concentration of 80 μg/mL was achieved. Taking into consideration the fact that the one eye drop of 1% ophthalmic solution contains 500 μg of voriconazole, it can be concluded that the hydrogel rings can be considered as an effective alternative since it releases the similar amount of drug (250-800 μg) in a more sustainable way providing higher bioavailability.

Although this new drug delivery device offers the advantage efficacy in comparison with regular eye drops, it is possible that hydrogel rings may result in complications due to toxicity (for epithelial cells, for instance) or other side effects. It is not likely that the polymer material will be causing problems due to toxicity or bio-incompatibility; hydrogels are used extensively in contact with ocular epithelium (soft contact lenses), and PVP is commonly used in ocular formulations. Complications may arise due to high local concentrations of the drug, especially at the epithelium-touching surface of the device. Prevention of such complications may require re-design of the device. Another important aspect that needs to be investigated thoroughly is the effect of the presence of the hydrogel ring on the flow of the tear fluid. Obviously, the ring will impede the flow in the direction of the upper and lower canaliculi. In addition, it is anticipated that there will be practically no flow in the inner circular of the ring. If this is the case indeed, then the absence of tear flow in the center of the ring may lead to enhanced bioavailability of the drug in the inner part of the ring, i.e., exactly at the site of the infection. All of this implies that much further research and development work, involving representative models of the tear flow at the ocular surface, is required. Preclinical testing using animal (rabbit) models for corneal infection, as well as clinical testing on human patients, will

subsequently be mandatory to convince the medical community of the effectiveness and safety of our drug-delivery concept.

Bibliography/References

[1] U. Jurkunas, I. Behlau, K. Colby, Fungal Keratitis: Changing Pathogens and Risk Factors, Cornea. 28 (2009) 638-643. doi:10.1097/ico.0b013e318191695b.

[2] M. Green, S. Sara, I. Hughes, A. Apel, F. Stapleton, Trends in contact lens microbial keratitis 1999 to 2015: a retrospective clinical review, Clinical & Experimental Ophthalmology. (2019). doi:10.1111/ceo.13484.

[3] P. Thomas, J. Kaliamurthy, Mycotic keratitis: epidemiology, diagnosis and management, Clinical Microbiology and Infection. 19 (2013) 210-220. doi:10.1111/1469-0691.12126.

[4] J. Huang, J. Zhong, G. Chen, Z. Lin, Y. Deng, Y. Liu et al., A Hydrogel-Based Hybrid Theranostic Contact Lens for Fungal Keratitis, ACS Nano. 10 (2016) 6464-6473. doi:10.1021/acsnano.6b00601.

[5] S. Hariprasad, W. Mieler, T. Lin, W. Sponsel, J. Graybill, Voriconazole in the treatment of fungal eye infections: a review of current literature, British Journal of Ophthalmology. 92 (2008) 871-878. doi:10.1136/bjo.2007.136515.

[6] M. Nejabat, N. Yaqubi, A. Khosravi, K. Zomorodian, M. Ashraf, R. Salouti, Therapeutic Effect of Intrastromal Voriconazole, Topical Voriconazole, and Topical Natamycin on Fusarium Keratitis in Rabbit, Journal of Ophthalmology. 2016 (2016) 1-6. doi:10.1155/2016/8692830.

[7] P. Shukla, M. Kumar, G. Keshava, Mycotic keratitis: an overview of diagnosis and therapy, Mycoses. 51 (2008) 183-199. doi:10.1111/j.1439-0507.2007.01480.x.

[8] Y. Mahmoud, Fungal Keratitis Efficient Treatments using Surface Active Agents (Cetrimide): an Overview, Journal Of Bacteriology & Mycology: Open Access. 2 (2016). doi:10.15406/jbmoa.2016.02.00026.

[9] N. Prajna, Comparison of Natamycin and Voriconazole for the Treatment of Fungal Keratitis, Archives of Ophthalmology. 128 (2010) 672. doi:10.1001/archophthalmol.2010.102.

[10] M. Hogan, J. Crawford, Epidemic Keratoconjunctivitis ∗ ∗From the Department of Ophthalmology, Division of Surgery, University of California Medical School, San

Francisco, USA., American Journal of Ophthalmology. 190 (2018) xxix-xlii. doi:10.1016/j.ajo.2018.03.041.

[11] E. McDonald, F. Ram, D. Patel, C. McGhee, Topical antibiotics for the management of bacterial keratitis: an evidence-based review of high quality randomized controlled trials, British Journal of Ophthalmology. 98 (2014) 1470-1477. doi:10.1136/bjophthalmol-2013-304660.

[12] M. Constantinou, M. Daniell, G. Snibson, H. Vu, H. Taylor, Clinical Efficacy of Moxifloxacin in the Treatment of Bacterial Keratitis, Ophthalmology. 114 (2007) 1622-1629. doi:10.1016/j.ophtha.2006.12.011.

[13] Z. Ansari, D. Miller, A. Galor, Current Thoughts in Fungal Keratitis: Diagnosis and Treatment, Current Fungal Infection Reports. 7 (2013) 209-218. doi:10.1007/s12281-013-0150-1.

[14] G. Müller, N. Kara-José, R. Castro, Antifungals in eye infections: drugs and routes of administration, Revista Brasileira De Oftalmologia. 72 (2013) 132-141. doi:10.1590/s0034-72802013000200014.

[15] T. Hiraoka, Y. Kaji, T. Wakabayashi, P. Nanbu, F. Okamoto, T. Oshika, Comparison of Micafungin and Fluconazole for Experimental Candida Keratitis in Rabbits, Cornea. 26 (2007) 336-342. doi:10.1097/ico.0b013e31802cd8a8.

[16] Y. Matsumoto, D. Murat, T. Kojima, J. Shimazaki, K. Tsubota, The comparison of solitary topical micafungin or fluconazole application in the treatment of Candida fungal keratitis, British Journal of Ophthalmology. 95 (2010) 1406-1409. doi:10.1136/bjo.2010.191734.

[17] S. Marasini, S. Swift, S. Dean, S. Ormonde, J. Craig, Spectrum and Sensitivity of Bacterial Keratitis Isolates in Auckland, Journal of Ophthalmology. 2016 (2016) 1-8. doi:10.1155/2016/3769341.

[18] V. Díaz-Tomé, A. Luaces-Rodríguez, J. Silva-Rodríguez, S. Blanco-Dorado, L. García-Quintanilla, J. Llovo-Taboada et al., Ophthalmic Econazole Hydrogels for the Treatment of Fungal Keratitis, Journal of Pharmaceutical Sciences. 107 (2018) 1342-1351. doi:10.1016/j.xphs.2017.12.028.

[19] W. Behrens-Baumann, B. Klinge, R. Ruchel, Topical fluconazole for experimental candida keratitis in rabbits., British Journal of Ophthalmology. 74 (1990) 40-42. doi:10.1136/bjo.74.1.40.

[20] Z. Wu, H. Ying, S. Yiu, J. Irvine, R. Smith, Fungal Keratitis Caused by Scedosporium Apiospermum, Cornea. 21 (2002) 519-523. doi:10.1097/00003226-200207000-00016.

[21] D. Al-Badriyeh, L. Lok, T. Roydhouse, J. Li, M. Daniell, R. Fullinfaw et al., 2% Voriconazole Eye Drops for the Management of Ophthalmic Fungal Keratitis, International Journal of Infectious Diseases. 12 (2008) e285. doi:10.1016/j.ijid.2008.05.764.

[22] Y. Ramesh, C. Kothapalli, J. Reddigari, A NOVEL APPROACHES ON OCULAR DRUG DELIVERY SYSTEM, Journal of Drug Delivery and Therapeutics. 7 (2017). doi:10.22270/jddt.v7i6.1512.

[23] Y. Ban, A. Dota, L. Cooper, N. Fullwood, T. Nakamura, M. Tsuzuki et al., Tight junction-related protein expression and distribution in human corneal epithelium, Experimental Eye Research. 76 (2003) 663-669. doi:10.1016/s0014-4835(03)00054-x.

[24] S. Garg, Drug delivery and targeting (for pharmacists and pharmaceutical scientists), Drug Discovery Today. 7 (2002) 858. doi:10.1016/s1359-6446(02)02366-8.

[25] S. Amrith, G. Sundar, S. Young, Ocular Adnexal Lesions, Springer, Singapore, 2019.

[26] A. Sharma, J. Taniguchi, Review: Emerging strategies for antimicrobial drug delivery to the ocular surface: Implications for infectious keratitis, The Ocular Surface. 15 (2017) 670-679. doi:10.1016/j.jtos.2017.06.001.

[27] S. Liu, L. Jones, F. Gu, Nanomaterials for Ocular Drug Delivery, Macromolecular Bioscience. 12 (2012) 608-620. doi:10.1002/mabi.201100419.

[28] L. Battaglia, L. Serpe, F. Foglietta, E. Muntoni, M. Gallarate, A. Del Pozo Rodriguez et al., Application of lipid nanoparticles to ocular drug delivery, Expert Opinion on Drug Delivery. 13 (2016) 1743-1757. doi:10.1080/17425247.2016.1201059.

[29] H. Almeida, M. Amaral, P. Lobao, C. Frigerio, J. Sousa Lobo, Nanoparticles in Ocular Drug Delivery Systems for Topical Administration: Promises and Challenges, Current

Pharmaceutical Design. 21 (2015) 5212-5224. doi:10.2174/1381612821666150923095155.

[30] S. Das, P. Suresh, Nanosuspension: a new vehicle for the improvement of the delivery of drugs to the ocular surface. Application to amphotericin B, Nanomedicine: Nanotechnology, Biology and Medicine. 7 (2011) 242-247. doi:10.1016/j.nano.2010.07.003.

[31] H. Ibrahim, I. El-Leithy, A. Makky, Mucoadhesive Nanoparticles as Carrier Systems for Prolonged Ocular Delivery of Gatifloxacin/Prednisolone Bitherapy, Molecular Pharmaceutics. 7 (2010) 576-585. doi:10.1021/mp900279c.

[32] S. Song, W. Zhou, Y. Wang, J. Jian, Self-aggregated nanoparticles based on amphiphilic poly(lactic acid)-grafted-chitosan copolymer for ocular delivery of amphotericin B, International Journal Of Nanomedicine. (2013) 3715. doi:10.2147/ijn.s51186.

[33] Y. Chhonker, Y. Prasad, H. Chandasana, A. Vishvkarma, K. Mitra, P. Shukla et al., Amphotericin-B entrapped lecithin/chitosan nanoparticles for prolonged ocular application, International Journal of Biological Macromolecules. 72 (2015) 1451-1458. doi:10.1016/j.ijbiomac.2014.10.014.

[34] A. Mahmoud, G. El-Feky, R. Kamel, G. Awad, Chitosan/sulfobutylether-β-cyclodextrin nanoparticles as a potential approach for ocular drug delivery, International Journal of Pharmaceutics. 413 (2011) 229-236. doi:10.1016/j.ijpharm.2011.04.031.

[35] R. Bhatta, H. Chandasana, Y. Chhonker, C. Rathi, D. Kumar, K. Mitra et al., Mucoadhesive nanoparticles for prolonged ocular delivery of natamycin: In vitro and pharmacokinetics studies, International Journal of Pharmaceutics. 432 (2012) 105-112. doi:10.1016/j.ijpharm.2012.04.060.

[36] H. Gupta, M. Aqil, R. Khar, A. Ali, A. Bhatnagar, G. Mittal, Biodegradable levofloxacin nanoparticles for sustained ocular drug delivery, Journal of Drug Targeting. 19 (2010) 409-417. doi:10.3109/1061186x.2010.504268.

[37] M. Kalam, Y. Sultana, A. Ali, M. Aqil, A. Mishra, I. Aljuffali et al., Part I: Development and optimization of solid-lipid nanoparticles using Box-Behnken statistical design for ocular delivery of gatifloxacin, Journal Of Biomedical Materials Research Part A. 101A (2012) 1813-1827. doi:10.1002/jbm.a.34453.

[38] R. Cavalli, M. Gasco, P. Chetoni, S. Burgalassi, M. Saettone, Solid lipid nanoparticles (SLN) as ocular delivery system for tobramycin, International Journal of Pharmaceutics. 238 (2002) 241-245. doi:10.1016/s0378-5173(02)00080-7.

[39] S. MOTWANI, S. CHOPRA, S. TALEGAONKAR, K. KOHLI, F. AHMAD, R. KHAR, Chitosan–sodium alginate nanoparticles as submicroscopic reservoirs for ocular delivery: Formulation, optimisation and in vitro characterisation, European Journal of Pharmaceutics and Biopharmaceutics. (2007). doi:10.1016/j.ejpb.2007.09.009.

[40] A. Seyfoddin, J. Shaw, R. Al-Kassas, Solid lipid nanoparticles for ocular drug delivery, Drug Delivery. 17 (2010) 467-489. doi:10.3109/10717544.2010.483257.

[41] I. Carvalho, C. Marques, R. Oliveira, P. Coelho, P. Costa, D. Ferreira, Sustained drug release by contact lenses for glaucoma treatment—A review, Journal of Controlled Release. 202 (2015) 76-82. doi:10.1016/j.jconrel.2015.01.023.

[42] A. Hui, A. Boone, L. Jones, Uptake and Release of Ciprofloxacin-HCl From Conventional and Silicone Hydrogel Contact Lens Materials, Eye & Contact Lens: Science & Clinical Practice. 34 (2008) 266-271. doi:10.1097/icl.0b013e3181812ba2.

[43] C. Phan, L. Subbaraman, L. Jones, Contact lenses for antifungal ocular drug delivery: a review, Expert Opinion on Drug Delivery. 11 (2014) 537-546. doi:10.1517/17425247.2014.882315.

[44] M. Bajgrowicz, C. Phan, L. Subbaraman, L. Jones, Release of Ciprofloxacin and Moxifloxacin from Daily Disposable Contact Lenses from an In Vitro Eye Model, Investigative Ophthalmology & Visual Science. 56 (2015) 2234. doi:10.1167/iovs.15-16379.

[45] M. Busin, M. Spitznas, Sustained Gentamicin Release by Presoaked Medicated Bandage Contact Lenses, Ophthalmology. 95 (1988) 796-798. doi:10.1016/s0161-6420(88)33106-4.

[46] A. Hui, M. Willcox, L. Jones, In Vitro and In Vivo Evaluation of Novel Ciprofloxacin-Releasing Silicone Hydrogel Contact Lenses, Investigative Ophthalmology & Visual Science. 55 (2014) 4896. doi:10.1167/iovs.14-14855.

[47] P. Paradiso, A. Serro, B. Saramago, R. Colaço, A. Chauhan, Controlled Release of Antibiotics from Vitamin E–Loaded Silicone-Hydrogel Contact Lenses, Journal of Pharmaceutical Sciences. 105 (2016) 1164-1172. doi:10.1016/s0022-3549(15)00193-8.

[48] C. Peng, J. Kim, A. Chauhan, Extended delivery of hydrophilic drugs from silicone-hydrogel contact lenses containing Vitamin E diffusion barriers, Biomaterials. 31 (2010) 4032-4047. doi:10.1016/j.biomaterials.2010.01.113.

[49] P. Paradiso, A. Serro, B. Saramago, R. Colaço, A. Chauhan, Controlled Release of Antibiotics from Vitamin E–Loaded Silicone-Hydrogel Contact Lenses, Journal of Pharmaceutical Sciences. 105 (2016) 1164-1172. doi:10.1016/s0022-3549(15)00193-8.

[50] S. Kirchhof, A. Goepferich, F. Brandl, Hydrogels in ophthalmic applications, European Journal of Pharmaceutics and Biopharmaceutics. 95 (2015) 227-238. doi:10.1016/j.ejpb.2015.05.016.

[51] S. Van Tomme, G. Storm, W. Hennink, In situ gelling hydrogels for pharmaceutical and biomedical applications, International Journal of Pharmaceutics. 355 (2008) 1-18. doi:10.1016/j.ijpharm.2008.01.057.

[52] D. Shastri, S. Prajapati, L. Patel, Design and Development of Thermoreversible Ophthalmic in Situ Hydrogel of Moxifloxacin HCl, Current Drug Delivery. 7 (2010) 238-243. doi:10.2174/156720110791560928.

[53] B. Nanjwade, R. Deshmukh, K. Gaikwad, K. Parikh, F. Manvi, Formulation and evaluation of micro hydrogel of Moxifloxacin hydrochloride, European Journal of Drug Metabolism and Pharmacokinetics. 37 (2011) 117-123. doi:10.1007/s13318-011-0070-9.

[54] Y. Chen, G. Cheng, R. Hu, S. Chen, W. Lu, S. Gao et al., A Nasal Temperature and pH Dual-Responsive in Situ Gel Delivery System Based on Microemulsion of Huperzine A: Formulation, Evaluation, and In Vivo Pharmacokinetic Study, AAPS Pharmscitech. 20 (2019). doi:10.1208/s12249-019-1513-x.

[55] G. Coneac, V. Vlaia, I. Olariu, A. Muţ, D. Anghel, C. Ilie et al., Development and Evaluation of New Microemulsion-Based Hydrogel Formulations for Topical Delivery of Fluconazole, AAPS Pharmscitech. 16 (2015) 889-904. doi:10.1208/s12249-014-0275-8.

[56] A. Malik, R. Khar, A. Ali, A. Bhatnagar, G. Mittal, H. Gupta, Physiologically active hydrogel (in situ gel) of sparfloxacin and its evaluation for ocular retention using gamma

scintigraphy, Journal of Pharmacy And Bioallied Sciences. 7 (2015) 195. doi:10.4103/0975-7406.160015.

[57] K. Kesavan, Sodium Alginate Based Mucoadhesive System for Gatifloxacin and Its In Vitro Antibacterial Activity, Scientia Pharmaceutica. 78 (2010) 941-957. doi:10.3797/scipharm.1004-24.

[58] P. Bártolo, Stereolithography, Springer, New York, 2011.

[59] D. Moore, J. Beck, R. Kryscio, An objective assessment of the variability in number of drops per bottle of glaucoma medication, BMC Ophthalmology. 17 (2017). doi:10.1186/s12886-017-0473-8.

[60] G Srinu Babu, Ch AI Raju, UV-Spectrophotometric Determination of Voriconazole in bulk and its formulation, Asian Journal of Chemistry 19.2 (2007): 1625-1627.

[61] N. Tamilselvi, UV-Spectrophotometric analysis of Voriconazole in tablet dosage form, Research Journal of Pharmacy and Technology 4.11 (2011): 1791-1793.

[62] R. Baswani and M. Mathrusri, New Spectrophotometric Methods for the Determination of Voriconazole – An Anti-Fungal Agent, Acta Scientific Pharmaceutical Sciences 3 (2019): 2581-5423.